G-2 Internal
Version 1.0
November 25, 2019

Cornell momentum time correlation study

J. Fagin[1], T. Barrett[1], A. Chapelain[1], D. Rubin[1], and D. Seleznev[1]
[1]Cornell University

Abstract

The form of a momentum time correlation for real data is unknown, but we know it will be small enough that we can approximate it as a third degree polynomial for implementation in Monte Carlo. When a momentum time correlation is introduced, the symmetry point to begin the cosine transform will no longer be in the first turn of the fast rotation signal, but instead at the time when the muon beam is maximally debunched. We show how to find this point for a Gaussian frequency distribution and longitudinal beam by fitting the upper envelope of the fast rotation signal with the sum of three Gaussians. This will cause the max of the fitted function to be approximately the point of symmetry, which we can then use as the starting point for the cosine transform.

We also show how the true frequency distribution of the Monte Carlo changes when a momentum time correlation is introduced, since it will be the sum of the frequency distribution shifted by the location in the longitudinal beam profile. For a Gaussian frequency distribution and longitudinal beam profile, we show analytically how a linear correlation increases the width of the true frequency while the mean remains the same.

Contents

1 Introduction

For real data, the kicker can cause there to be a small correlation between the longitudinal beam profile and the radial distributions of the muons in the ring. This causes the the location of a muon in the longitudinal beam profile to affect its contribution to the radial position. The tail of the muon beam will have a higher or lower momentum than the muons at the head of the beam. We want to include this correlation into our analytical description of the fast rotation signal so that we can model this phenomenon with Monte Carlo.

If the kicker does provide a significant momentum time correlation to the muon beam, we know that it must be small. Since it is small and the form of the correlation is unknown, we assume a polynomial correlation between the frequency distribution and longitudinal beam profile since we can Taylor expand any correlation function to be approximately a polynomial in the region that the muon beam is within the collimator aperture.

2 Analytical description

2.1 Description of the fast rotation signal

We derived [1] the analytical form of the fast rotation signal S(t) without noise for a given frequency distribution $\rho(\Delta)$ and longitudinal beam profile $\xi(t)$ to be:

$$S(t) = \sum_{n=0}^{\infty} \int_{-\infty}^{\infty} \xi(t\prime) \frac{\rho(\frac{t-t\prime}{nT+t_0} - 1)}{nT + t_0} dt\prime = \sum_{n=\lfloor t\omega^- \rfloor}^{\lceil t\omega^+ \rceil} \int_{t-(1+\Delta_c)(nT+t_0)}^{t-(1-\Delta_c)(nT+t_0)} \xi(t\prime) \frac{\rho(\frac{t-t\prime}{nT+t_0} - 1)}{nT + t_0} dt\prime. \tag{1}$$

We can add a correlation between the longitudinal beam profile ξ and the frequency distribution ρ by changing the argument of ρ such that the frequency distribution is correlated to where in the longitudinal beam profile we are drawing from. For real data we expect the correlation to be small with a value somewhere between $\pm 0.15\%$, so we can Taylor expand the correlation between the longitudinal beam profile and the frequency distribution to approximate it by a polynomial as follows:

$$S(t) = \sum_{n=\lfloor t\omega^- \rfloor}^{\lceil t\omega^+ \rceil} \int_{t-(1+\Delta_c)(nT+t_0)}^{t-(1-\Delta_c)(nT+t_0)} \xi(t\prime) \frac{\rho\left(\frac{t-t\prime}{nT+t_0} - 1 + \sum_{k=1}^{N} r_k (\frac{t\prime - t_\xi}{T})^k\right)}{nT + t_0} dt\prime, \tag{2}$$

where r_k is the amplitude of the correlation and t_ξ is the mean of the longitudinal beam profile ξ so that the correlation has no effect on the frequency distribution when $t\prime = t_\xi$ as we would expect. For real data we expect that the correlation is between $\pm 0.15\%$ which is small enough so that a degree 3 polynomial is sufficient to represent all possible correlations so we can set the value of N to be 3.

2.2 Description of the frequency distribution

When we add a correlation between the frequency distribution and the longitudinal beam profile, we change the recovered frequency distribution since we are changing the mean of the frequency distribution depending on the location of the longitudinal beam profile. The relative amplitude of the frequency distribution is determined by the value of the longitudinal beam profile at that location. The true frequency distribution is the sum of all the frequency distributions for each location of the longitudinal beam profile with the amplitude determined by the longitudinal beam profile at that point. When this is done continuously for all points we integrate over all possible points in the longitudinal beam profile like the following equation:

$$\rho\prime(\Delta) = \int_{-\infty}^{\infty} \xi(t\prime)\rho\big(\Delta + \sum_{k=1}^{N} r_k(\frac{t\prime - t_\xi}{T})^k\big)dt\prime, \tag{3}$$

where $\rho\prime$ is the true frequency distribution and ρ is the originally chosen frequency distribution who's mean is shifted for each value of $t\prime$. When we generate a fast rotation signal and then use the Fourier method [2] to recover the frequency distribution, we will use $\rho\prime$ instead of ρ since $\rho\prime$ is the true frequency distribution.

3 Gaussian frequency distribution

3.1 Analytic derivation for linear momentum-time correlation

If we assume a Gaussian frequency distribution and longitudinal beam profile such that:

$$\rho(\Delta) = \frac{1}{\sqrt{2\pi\sigma_\rho}} e^{-\frac{(\Delta-\Delta_\rho)^2}{2\sigma_\rho^2}} \quad \text{and} \quad \xi(t) = \frac{1}{\sqrt{2\pi\sigma_\xi}} e^{-\frac{(t-t_\xi)^2}{2\sigma_\xi^2}}, \tag{4}$$

where Δ_ρ is the mean and σ_ρ is the standard deviation of the frequency distribution and t_ξ is the mean and σ_ξ is the standard deviation of the longitudinal beam profile. To demonstrate how the frequency distribution will change when a momentum-time correlation is added to the fast rotation signal, here we will assume a linear correlation so that we can get an analytic solution. For a linear momentum-time correlation, the true frequency distribution takes the following form:

$$\rho\prime(\Delta) = \int_{-\infty}^{\infty} \xi(t\prime)\rho\big(\Delta + r\frac{t\prime - t_\xi}{T}\big)dt\prime, \tag{5}$$

and then we can plug in the Gaussian frequency distributions and longitudinal beam profiles defined in equation 4 as follows:

$$\begin{aligned} \rho\prime(\Delta) &= \int_{-\infty}^{\infty} \frac{1}{\sqrt{2\pi\sigma_\xi}} e^{-\frac{(t-t_\xi)^2}{2\sigma_\xi^2}} \frac{1}{\sqrt{2\pi\sigma_\rho}} e^{-\frac{(\Delta-\Delta_\rho+r\frac{t\prime-t_\xi}{T})^2}{2\sigma_\rho^2}} dt\prime \\ &= \frac{1}{2\pi\sigma_\xi\sigma_\rho} \int_{-\infty}^{\infty} e^{-[(\frac{1}{2\sigma_\xi^2}+\frac{r^2}{2\sigma_\rho^2T^2})(t\prime-t_\xi)+\frac{2r(\Delta-\Delta_\rho)}{2\sigma_\rho^2T}(t\prime-t_\xi)+\frac{(\Delta-\Delta_\rho)}{2\sigma_\rho^2}]} dt\prime. \end{aligned} \tag{6}$$

This integral is in the form of a standard Gaussian integral so it can be evaluated as follows:

$$\rho\prime(\Delta) = \frac{1}{2\pi\sigma_\xi\sigma_\rho}\sqrt{\frac{\pi}{(\frac{1}{2\sigma_\xi^2}+\frac{r^2}{2\sigma_\rho^2T^2})}}e^{\frac{(\frac{r}{T\sigma_\rho^2})^2(\Delta-\Delta_\rho)^2}{4(\frac{1}{2\sigma_\xi^2}+\frac{r^2}{2\sigma_\rho^2T^2})}-\frac{(\Delta-\Delta_\rho)^2}{2\sigma_\rho^2}}, \tag{7}$$

which simplifies to:

$$\rho\prime(\Delta) = \frac{1}{\sqrt{2\pi(\sigma_\rho^2+\frac{r^2}{T^2}\sigma_\xi^2)}}e^{-\frac{(\Delta-\Delta_\rho)^2}{2(\sigma_\rho^2+\frac{r^2}{T^2}\sigma_\xi^2))}}. \tag{8}$$

The true frequency distribution still takes the form of a Gaussian, but with a new standard deviation:

$$\sigma_{\rho\prime} = \sqrt{\sigma_\rho^2+\frac{r^2}{T^2}\sigma_\xi^2} = \sigma_\rho\sqrt{1+\frac{r^2}{T^2}\frac{\sigma_\xi^2}{\sigma_\rho^2}} \tag{9}$$

and the new standard deviation always increases since $\frac{r^2}{T^2}\frac{\sigma_\xi^2}{\sigma_\rho^2} \geq 0$. If r is negative, then the standard deviation still increases so the true frequency distribution does not change if r changes sign but the fast rotation signal does.

For real data we expect $|r| \leq 0.15\%$, so we can Taylor expand our expression for the standard deviation of a Gaussian frequency distribution we got in equation (9) since $\frac{r^2}{T^2}\frac{\sigma_\xi^2}{\sigma_\rho^2} \ll 1$. The square root then becomes:

$$\sigma_{\rho\prime} = \sigma_\rho\sqrt{1+\frac{r^2}{T^2}\frac{\sigma_\xi^2}{\sigma_\rho^2}} \approx \sigma_\rho\big(1+\frac{1}{2}\frac{r^2}{T^2}\frac{\sigma_\xi^2}{\sigma_\rho^2}\big), \tag{10}$$

and the difference in the standard deviation $\Delta\sigma_\rho = \sigma_{\rho\prime} - \sigma_\rho$ then has the approximate expression:

$$\Delta\sigma_\rho \approx \frac{1}{2}\big(\frac{r\sigma_\xi}{T\sigma_\rho}\big)^2. \tag{11}$$

We can approximate complicated frequency distributions as a sum of Gaussians so we expect that the frequency distribution will simply widen when a linear correlation is introduced. This is unsurprising since the correlation is just summing the frequency distribution with shifted mean which would have to sum to some wider distribution. If the longitudinal beam profile was even like it is for the degree 2 polynomial, then the sum of the frequency distributions will be skewed to one side so the width will not increase evenly on each side of the frequency distribution and the form of the frequency distribution would no longer be preserved.

3.2 Numerical integration

In figure 1 we show a frequency distribution ρ centered at the magic frequency with a standard deviation of 5 kHz and a longitudinal beam profile ξ centered at zero with a standard deviation of 25 ns. We then numerically integrate the true frequency distribution by plugging ρ and ξ into equation (5). Figure 2 (a) shows 50 Gaussian frequency distributions with shifted means with a relative amplitude coming from the longitudinal beam profile between -T and T for r = 1%. Each Gaussian frequency distribution represents a time slice from equation (5). When we add all of the distributions up we obtain the true frequency distribution shown in figure 2 (b).

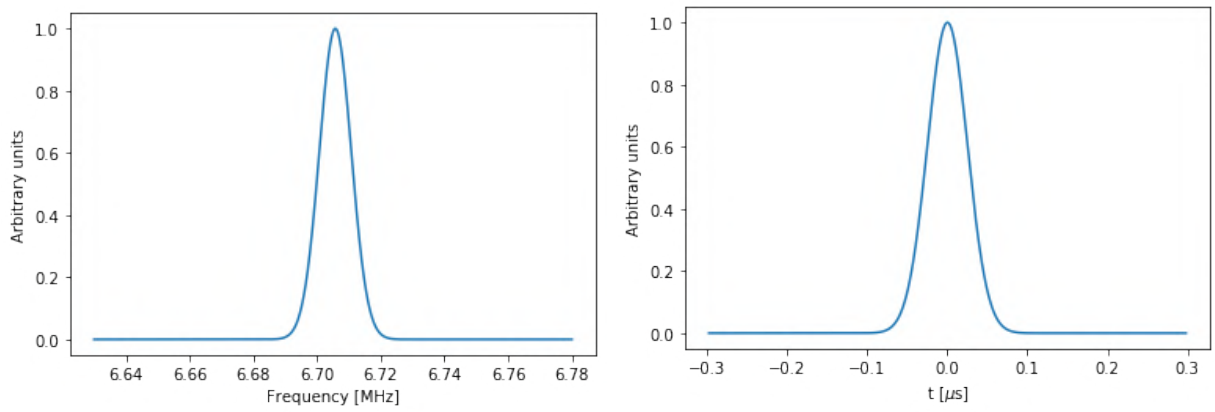

(a) (b)

Figure 1: A Gaussian frequency distribution and longitudinal beam: (a) frequency, (b) longitude.

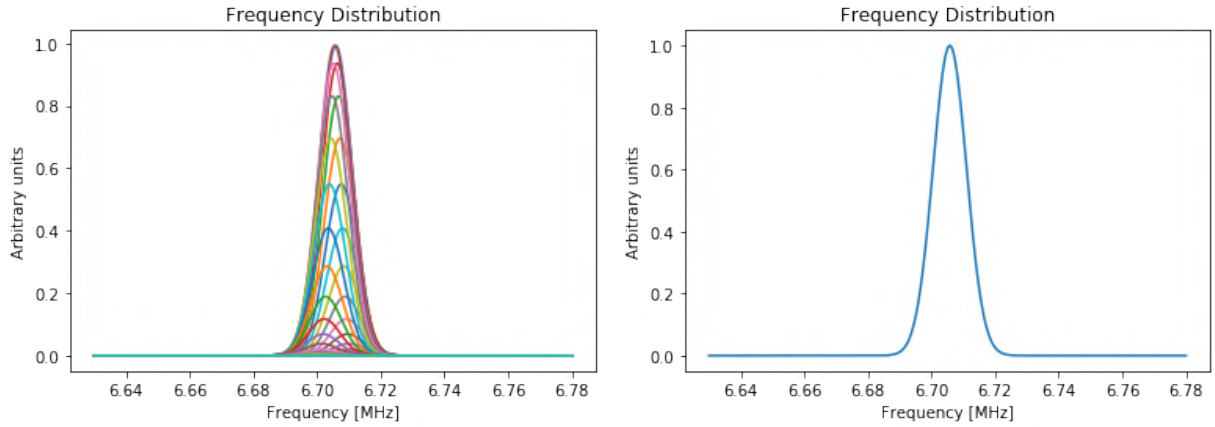

(a) (b)

Figure 2: We show the frequency distribution from 1 with center shifted and amplitude determined for the longitudinal beam profile for r = 1%: (a) shifted frequency distributions, (b) sum over shifted frequency distributions.

Figure 3 shows the true frequency distribution for different values of r found by numerically integrating original frequency distribution ρ into equation (5). We can clearly see the width of the frequency distribution increase with r which is what we expect from our derivation in equation (9). We overlay the frequency distributions in figure 4 so that we can see how when r is small the width of the frequency distribution does not change much, but for large r the width substantially increases.

Figure 5 shows the change in the mean, standard deviation, and E-field correction with r. We see in (a) that the mean does not change with r. On the other hand, the standard deviation increases proportionately to r^2 which matches the change in standard deviation we derived in equation (11). By extension the E-field correction gets more negative as well since it is negative and proportional in magnitude to the square of the standard deviation. Keep in mind that for real data, we expect the correlation to be around only 0.15% so we show here how change in the frequency distribution is very small for realistic correlations.

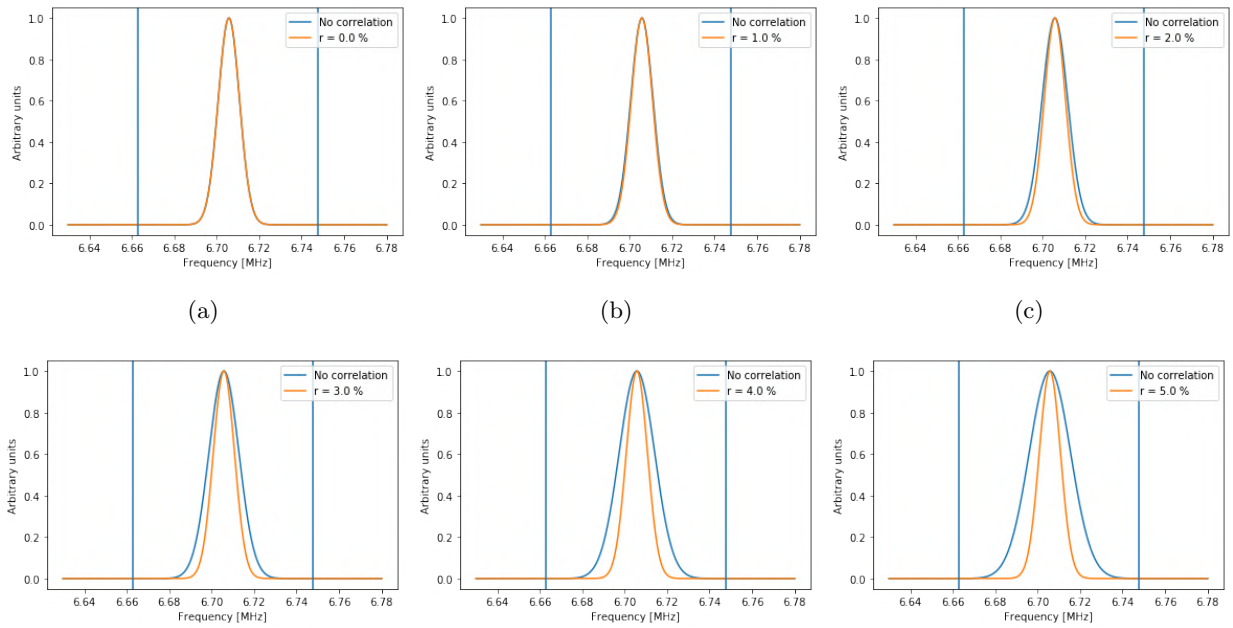

Figure 3: The change in the true frequency distribution with correlation for the frequency distribution and longitudinal beam profile shown in figure 1. Six values of r are shown: (a) r = 0%, (b) r = 1%, (c) r = 2%, (d) r = 3%, (e) r = 4%, (f) r = 5%.

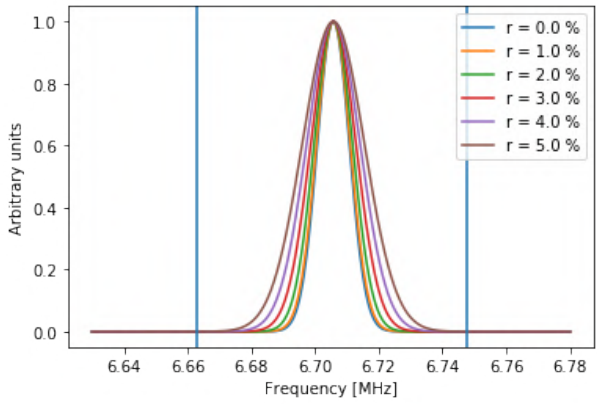

Figure 4: The change in the true frequency distribution with correlation overlaid for the frequency distribution and longitudinal beam profile shown in figure 1.

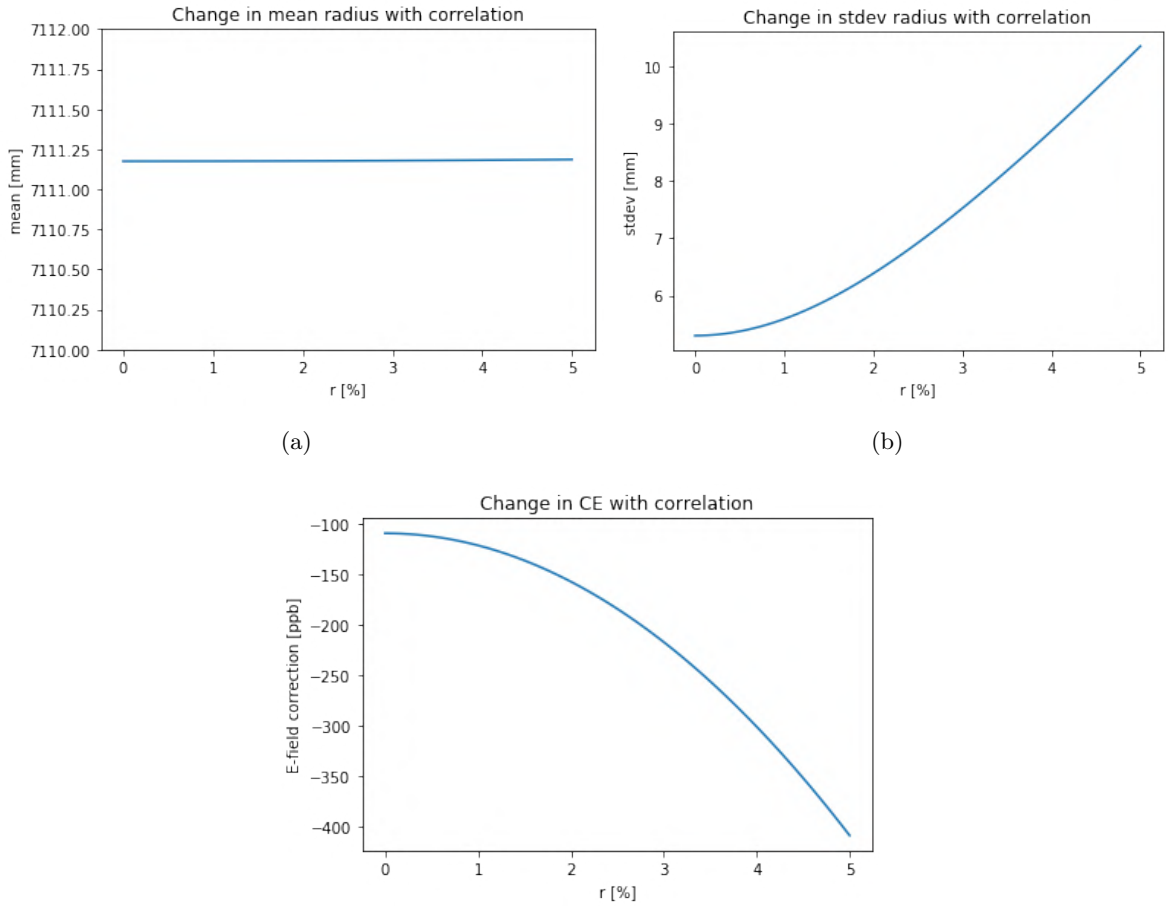

(a) (b)

(c)

Figure 5: The mean, stdev, and E-field correction vs r for the frequency distribution and longitudinal beam profile shown in figure 1: (a) mean, (b) stdev, (c) E-field.

4 Gaussian frequency distribution and beam profile Monte Carlo

4.1 Physical interpretation of the momentum time correlation

Here we show linear correlation between the frequency distribution and longitudinal beam profile using a Gaussian Monte Carlo fast rotation signal with no noise shown in figures 7,8,9. The values of the correlation are much higher that what we expect to see in real data, but by looking at these extreme cases we can demonstrate what the muon beam is doing. The frequency distribution is centered at the magic frequency with a fractional energy offset of 0.15% and the longitudinal beam profile is centered at 0 with a standard deviation of 25 ns shown in figure 6.

Shown in figures 7, 8,9 are the fast rotation signals generated by increasing linear momentum time correlations. The correlation is well past what we can expect in real data, but we can use these extreme examples to show how the correlation affects the fast rotation signal. We see in (a) of each figure that as the positive linear correlation increases, the peak of each distribution increases since the tail of the muon beam catches up to the head of the beam quicker so the muon beam reaches a peak concentration sooner before the beam has time to debunch. We can also see that for large momentum time correlations, we

can see multiple bumps throughout the fast rotation signal. These come from the tail of the muon beam catching up to the head of the beam multiple times around the ring.

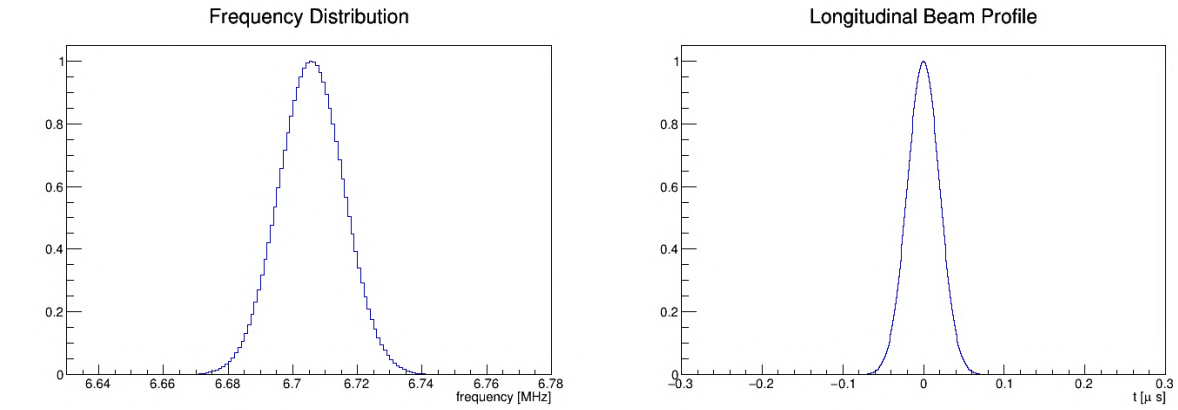

(a) (b)

Figure 6: The frequency distribution and longitudinal beam profile used to generate 7,8,9: (a) frequency, (b) longitude.

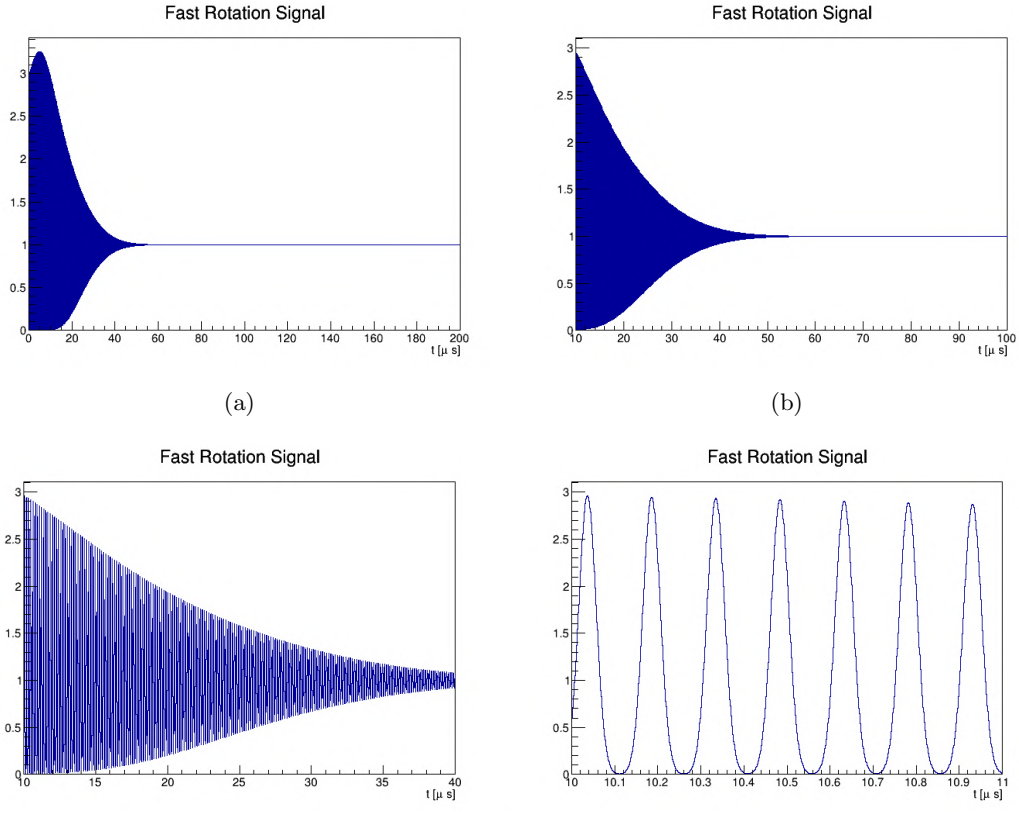

(a) (b)

(c) (d)

Figure 7: A fast rotation signal generated using a Monte Carlo simulation with r = 0.005. Four time intervals are shown: (a) 0-400 μs, (b) 10-100 μs, (c)10-40 μs, (d) 10-11 μs.

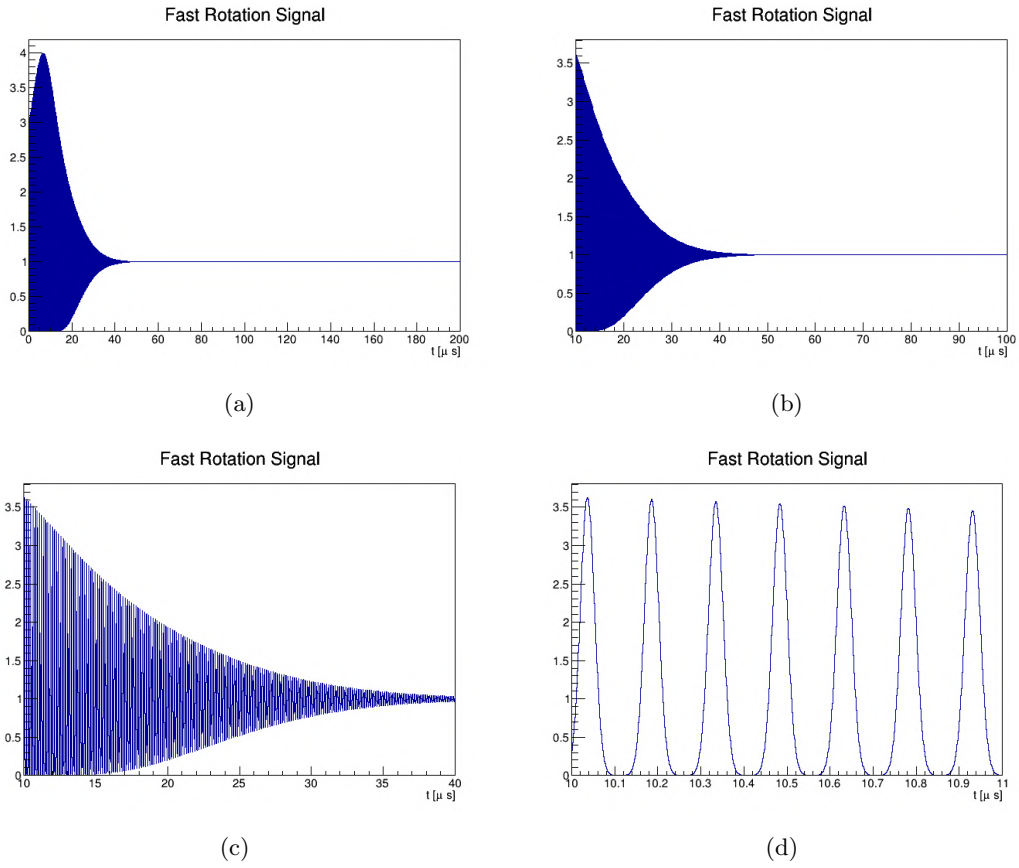

Figure 8: A fast rotation signal generated using a Monte Carlo simulation with r = 0.010. Four time intervals are shown: (a) 0-400 μs, (b) 10-100 μs, (c)10-40 μs, (d) 10-11 μs.

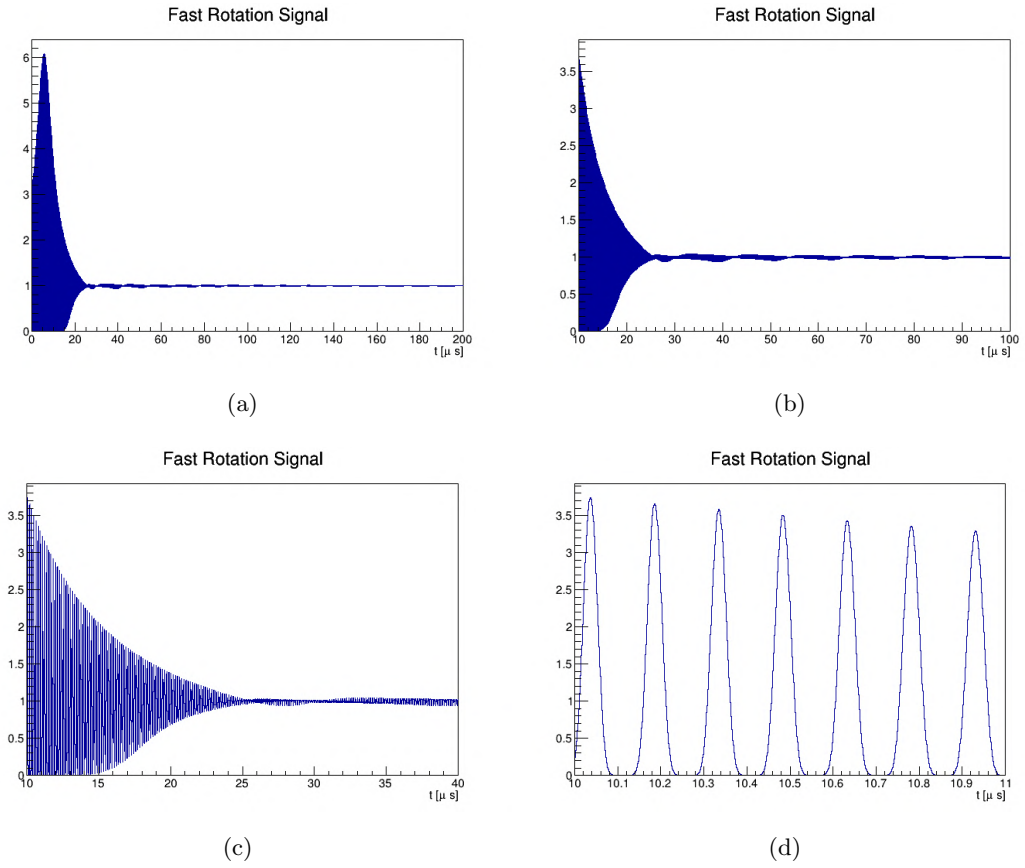

Figure 9: A fast rotation signal generated using a Monte Carlo simulation with r = 0.020. Four time intervals are shown: (a) 0-400 μs, (b) 10-100 μs, (c)10-40 μs, (d) 10-11 μs.

4.2 Correlation Scan at first turn

We must choose the right place to start the cosine transform of the fast rotation signal in order to correctly recover the radial distribution. The start time t_0 of the cosine transform represents the symmetry point where the muon beam is minimally debunched. This corresponds to the peak of the fast rotation signal where the muon beam is at its tightest spread. The start time t_0 is periodic with period T, the magic period, so we need to optimize the correct value of t_0 from $\pm$T/2 of the peak of the fast rotation signal.

The problem is that for real data, due to the beam line positron contamination of the muon beam we are unable to see the peak of the fast rotation signal if it occurs between 0-4 μs. Furthermore, if the momentum time correlation is negative, then that peak will occur at negative time before the signal even began since a negative momentum time correlation is as if the muon beam has debunched before the muons enter the ring. This makes it difficult to know where the peak of the fast rotation signal is for real data.

Shown in figure 10 is a fast rotation signal with a negative 0.15% linear momentum time correlation. This is the worst case scenario for a negative correlation. If we begin the analysis optimizing t_0 within the first period of the signal as if there is no correlation, then we can see in (d) that the mean of the radial distribution is correctly found within 0.15 mm, but the standard deviation is larger by more than 1.5 mm. This discrepancy leads to over a 100 ppb difference in recovered and actual E-field correction. Note that we use a value of the field index, n = 0.1075 to match the run-1 60-hour data set.

When the correlation is removed as in figure 11, this is no longer the case and the E-field correction is found to be within just 4 ppb since the t_0 used is now correct since the peak of the fast rotation signal must occur in the first period. When the correlation is positive 0.15% as in the opposite extreme case, the standard deviation of the recovered radial distribution is found to be more than 1 mm less than the actual standard deviation. This leads to more than a 100 ppb difference in the E-field correction, now in the opposite direction from the negative correlation.

We show in figure 13 that this effect is generalized when we do a scan over linear momentum correlation and difference in mean radius, standard deviation, and E-field correction. The mean radius varies only by small amounts coming from systematic uncertainty not from the wrong start time, while the standard deviation and E-field correction both have large linearly variations.

If we were not using a non-linear model for the correlation as we expect for real data, then the mean radius would no longer be recovered properly. Instead both the standard deviation and mean radius will vary since the correlation will no longer affect the head and the tail of the muon beam evenly but with opposite effects.

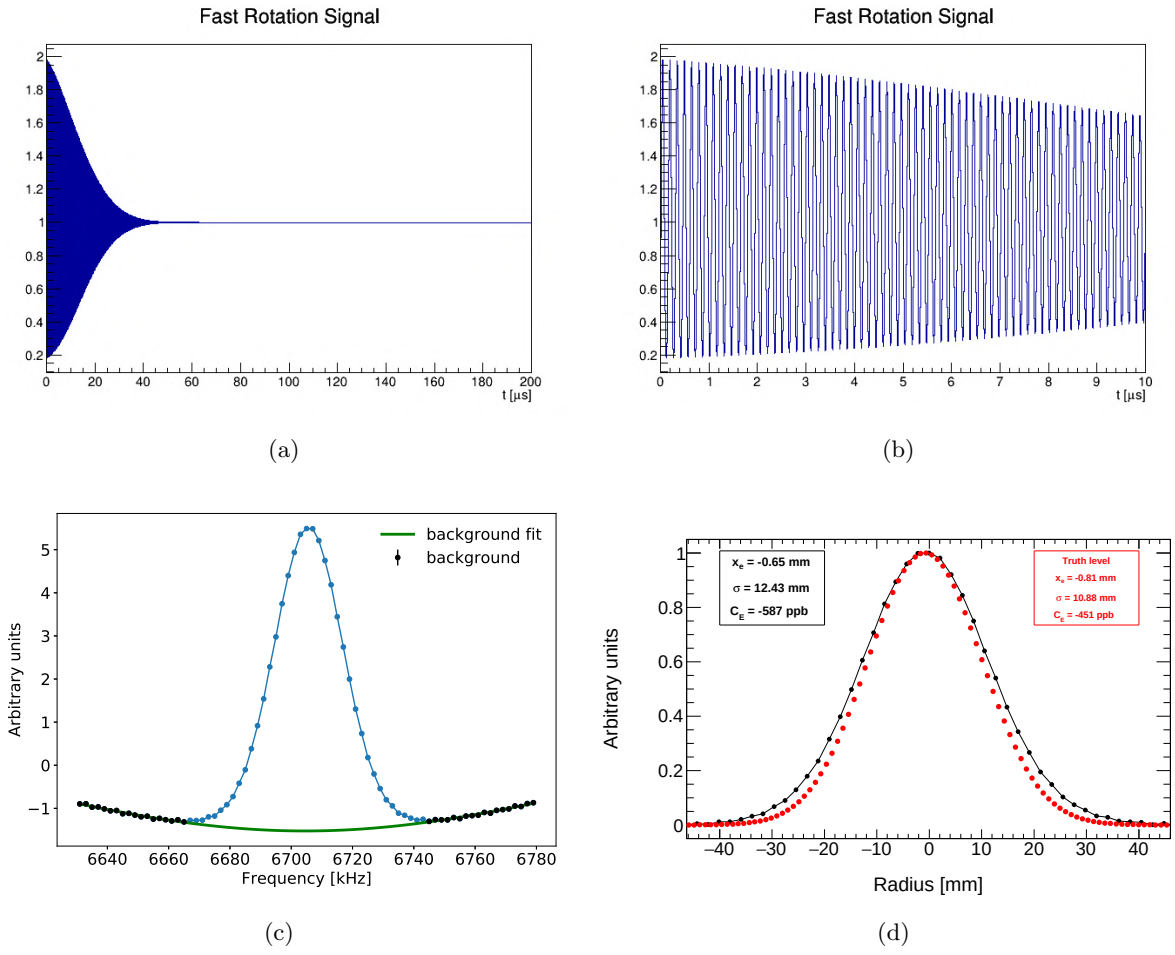

Figure 10: Fourier analysis of a fast rotation signal with Gaussian frequency distribution and longitudinal beam profile and a linear momentum time correlation of -0.15%. (a) fast rotation signal 0-200 μs, (b) fast rotation signal 0-10 μs, (c)background fit, (d) recovered radial distribution.

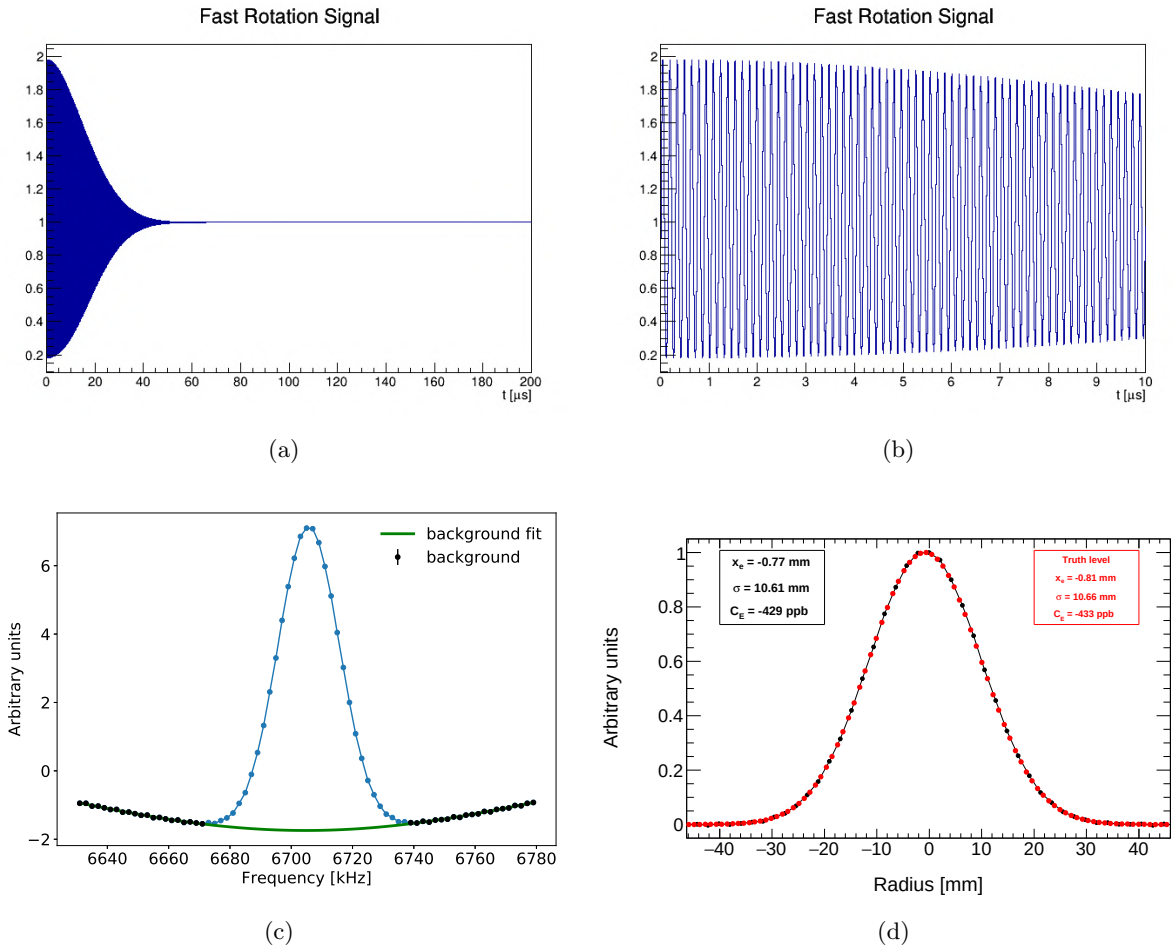

Figure 11: Fourier analysis of a fast rotation signal with Gaussian frequency distribution and longitudinal beam profile and no correlation. (a) fast rotation signal 0-200 μs, (b) fast rotation signal 0-10 μs, (c)background fit, (d) recovered radial distribution.

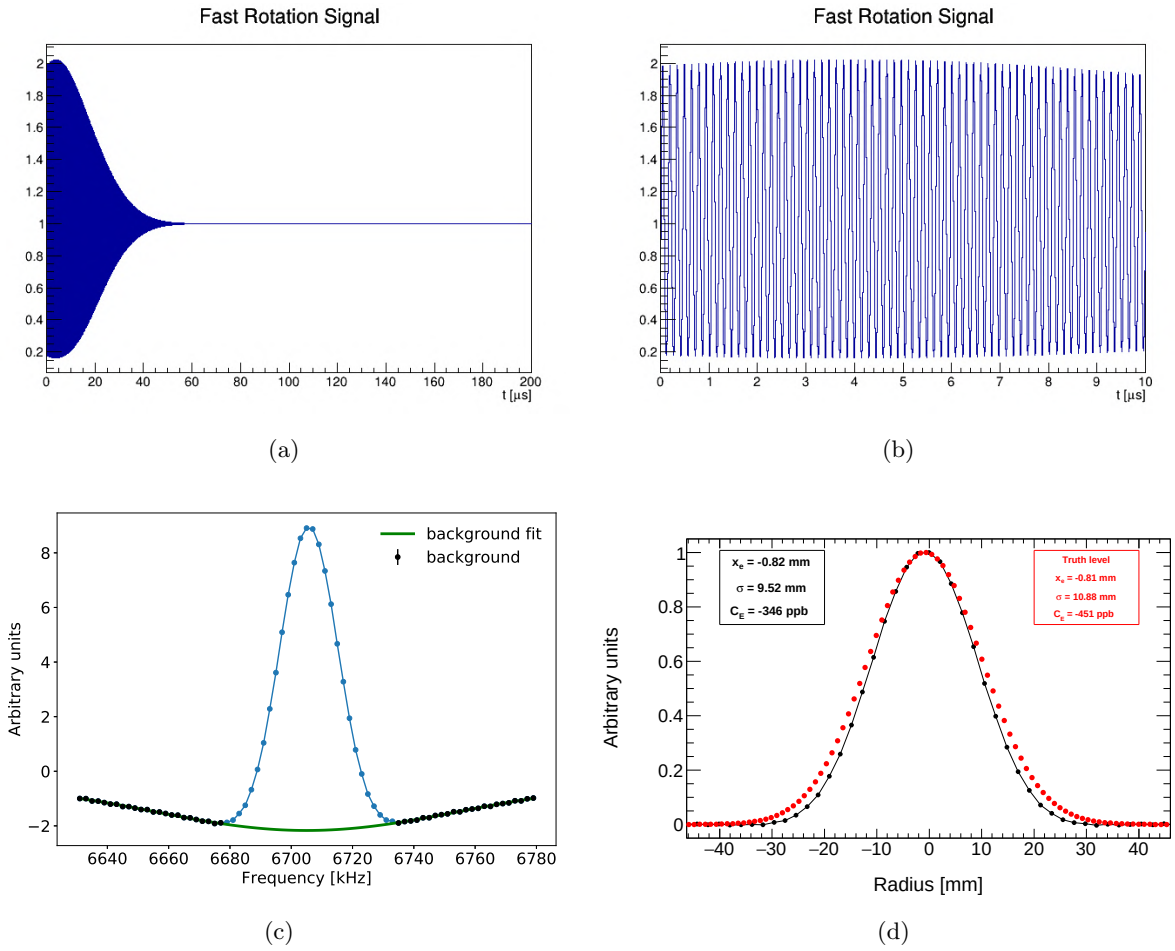

Figure 12: Fourier analysis of a fast rotation signal with Gaussian frequency distribution and longitudinal beam profile and a linear momentum time correlation of 0.15%. (a) fast rotation signal 0-200 μs, (b) fast rotation signal 0-10 μs, (c)background fit, (d) recovered radial distribution.

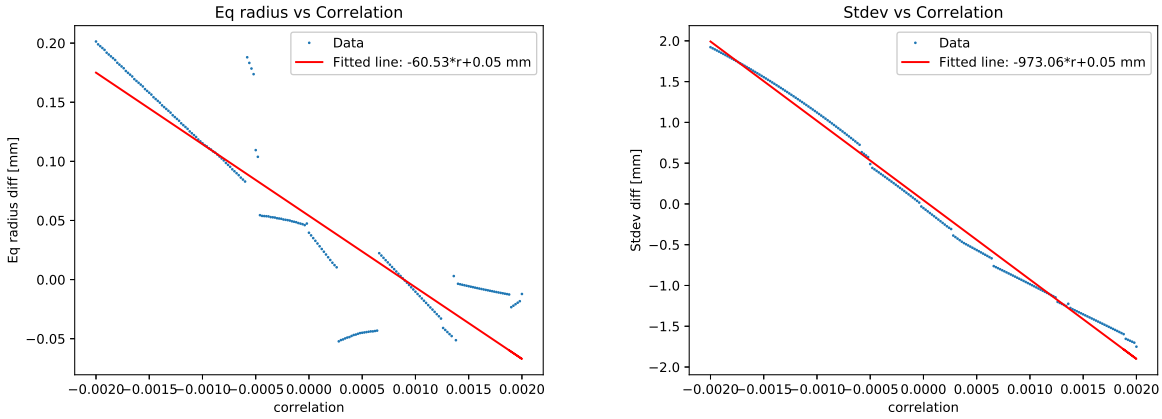

(a)

(b)

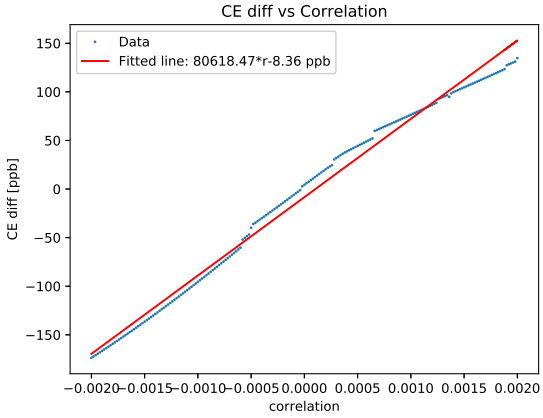

(c)

Figure 13: A scan over a linear momentum time correlation with Gaussian frequency distribution and longitudinal beam profile. Shown here are the difference between the recovered and actual (a) radial distribution [mm], (b) standard deviation [mm], (c) E-field correction. A linear fit is also done for each of the figures.

4.3 Correlation scan using optimized t_0 at max turn

The momentum time correlation changes the symmetry of the fast rotation signal. When a momentum time correlation is introduced, we no longer expect the correct cosine transform to begin in the first turn, because the cosine transform should start when the muon beam is maximally debunched.

In the real data there is beam-line contamination of the muon beam which we have to discard. This occurs for approximately the first 4 μs, so if the maximum point of debunching was from 0 to 4 μs, there would be no way to see it in the real dataset. Additionally, there is the possibility that the momentum time correlation is in the negative time domain. This occurs for the case with a negative linear momentum time correlation. We have no information on the fast rotation signal in the negative time since it is non-physical.

To remedy this problem, we can fit the upper envelope of the fast rotation signal with the sum of three Gaussians and use the max value of the fit function as the approximate symmetry point of the fast

rotation signal. This fit function can then be extended to the negative time domain and within the area of beam-line positron contamination of the muon beam. We start the fit only after 4 μs to mimic the real data sets. The upper/lower envelopes of the fast rotation signal are found simply by finding the max/min values of the fast rotation signal for each cyclotron period. Only the upper envelope is used.

We use the sum of Gaussians since the Fourier transform of a Gaussian is also a Gaussian, so for a Gaussian frequency distribution we expect the envelope of the fast rotation signal to also be a Gaussian. We use the sum of three Gaussians to account for the fact that the true frequency distribution is not Gaussian, but can be approximated as the sum of Gaussians.

We plot the extreme cases of the +0.15% and -0.15% correlation. When we use the max value we now only have a max of 8 ppb difference in E-field correlation.

4.3.1 Linear correlation scan using optimized t_0 at max turn

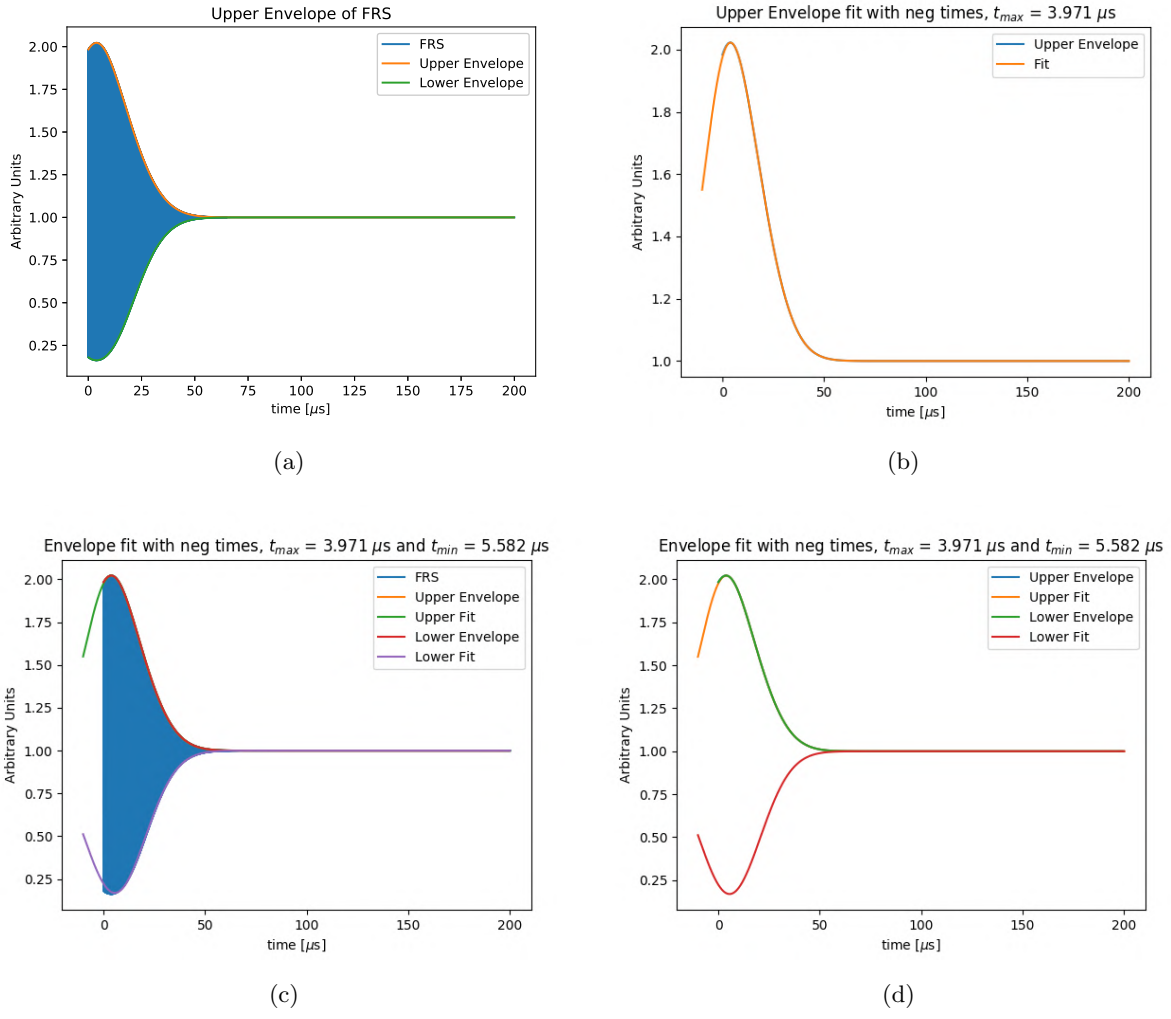

Figure 14: The envelope fit of the fast rotation signal for a linear correlation of 0.15%. (a) the upper and lower envelope and the FRS, (b) the upper envelope and the fit to it. (c) the upper and lower envelope and the fits together with the FRS, (d) the upper and lower envelope fits together.

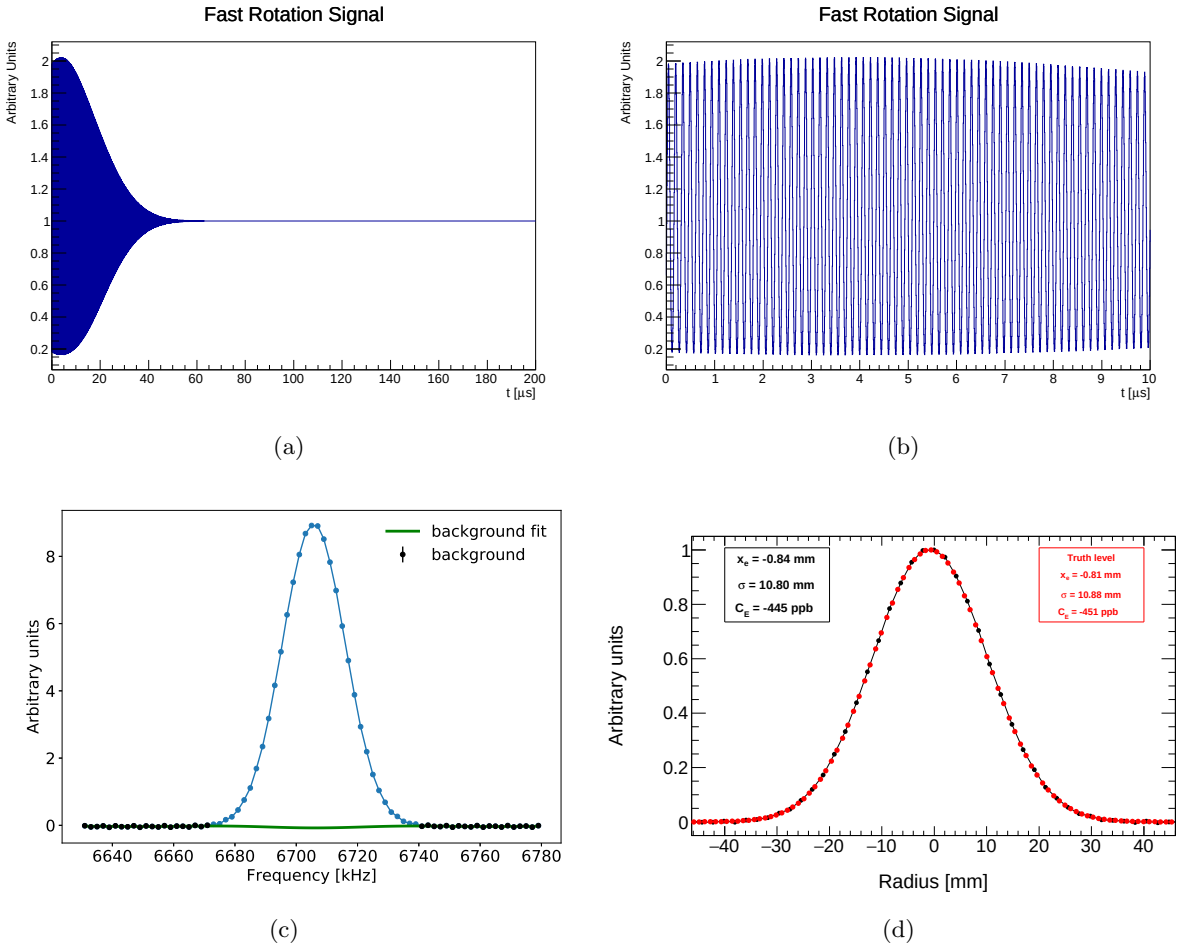

Figure 15: Fourier analysis of a fast rotation signal with Gaussian frequency distribution and longitudinal beam profile and a linear momentum time correlation of 0.15%. (a) fast rotation signal 0-200 μs, (b) fast rotation signal 0-10 μs, (c)background fit, (d) recovered radial distribution.

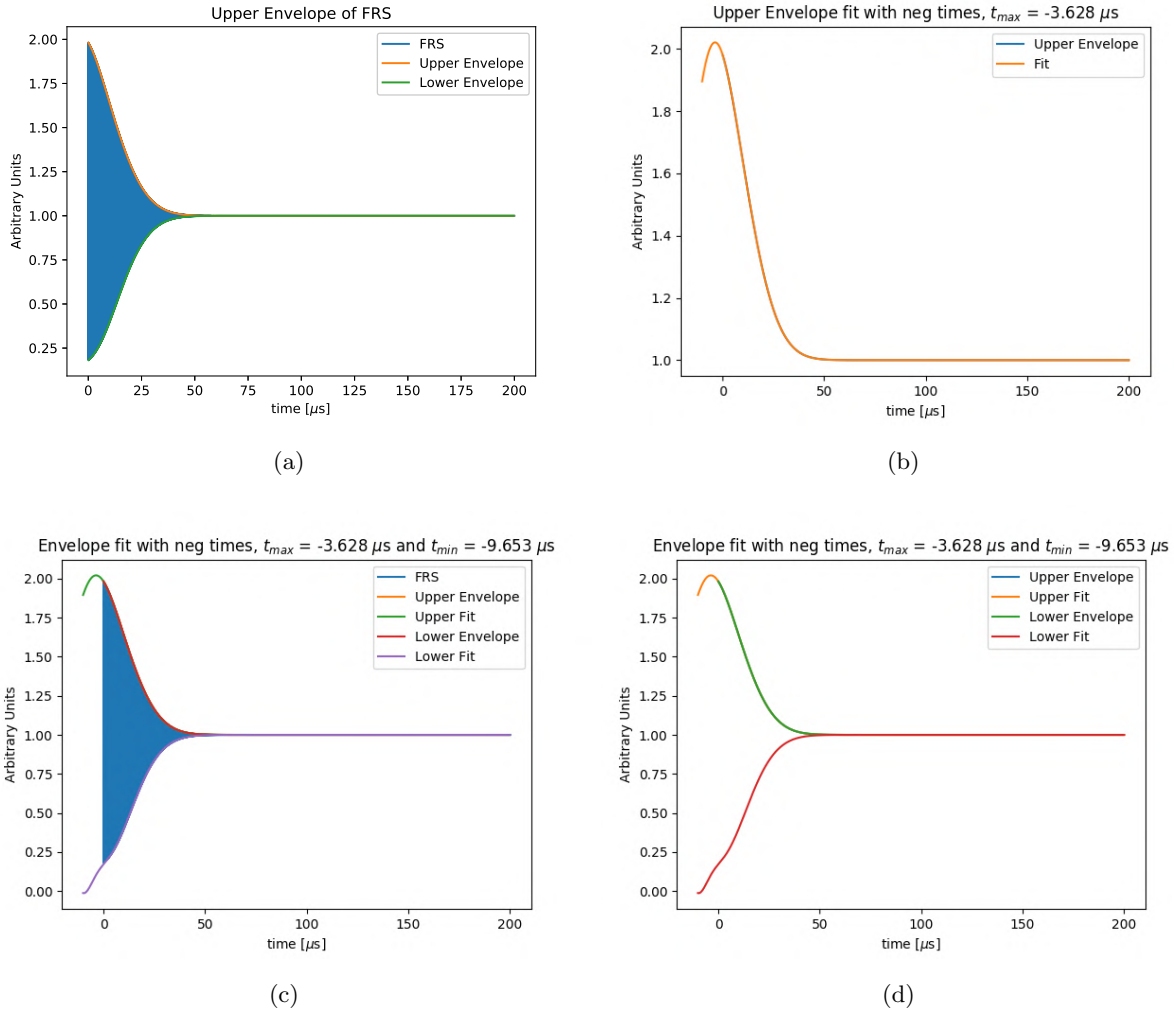

Figure 16: The envelope fit of the fast rotation signal for a linear correlation of -0.15%. (a) the upper and lower envelope and the FRS, (b) the upper envelope and the fit to it. (c) the upper and lower envelope and the fits together with the FRS, (d) the upper and lower envelope fits together.

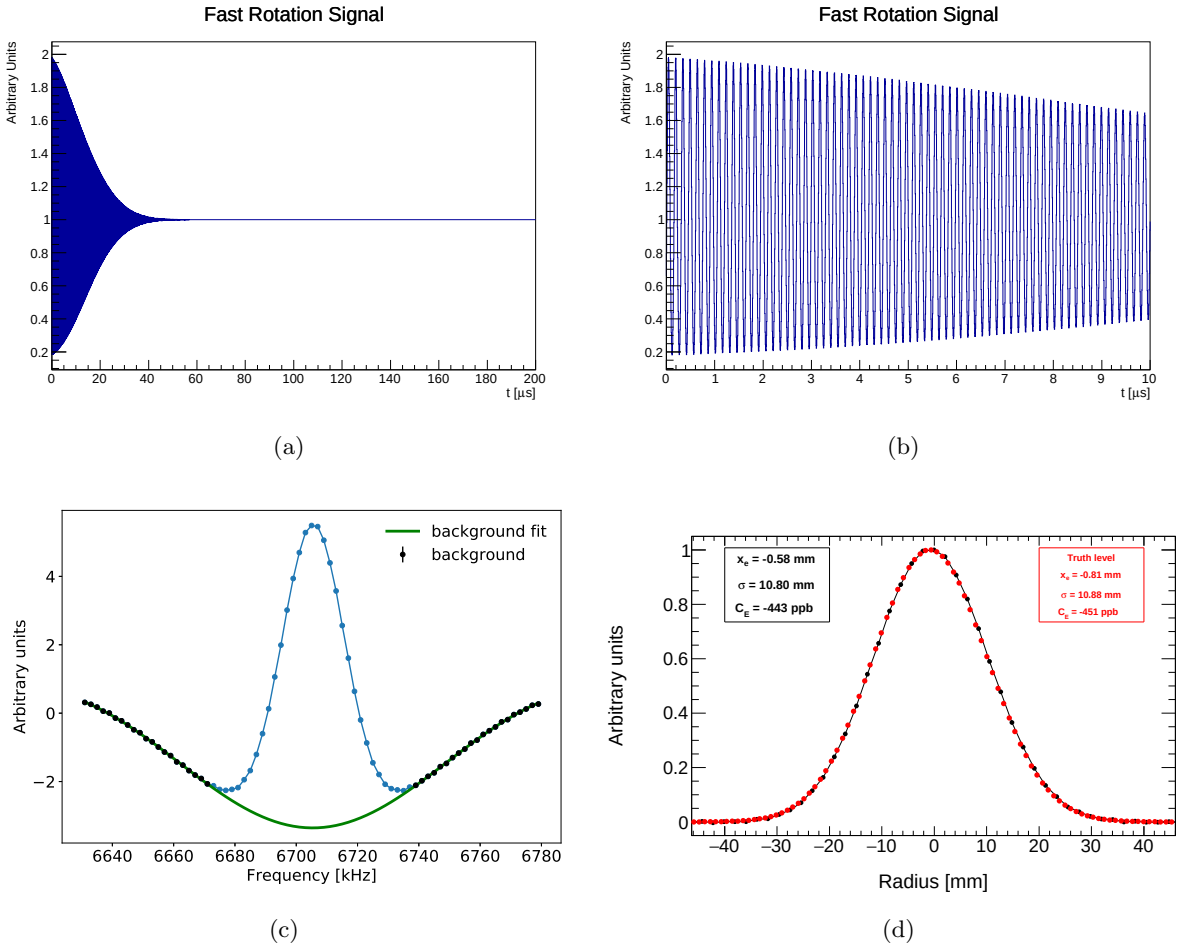

Figure 17: Fourier analysis of a fast rotation signal with Gaussian frequency distribution and longitudinal beam profile and a linear momentum time correlation of -0.15%. (a) fast rotation signal 0-200 μs, (b) fast rotation signal 0-10 μs, (c)background fit, (d) recovered radial distribution.

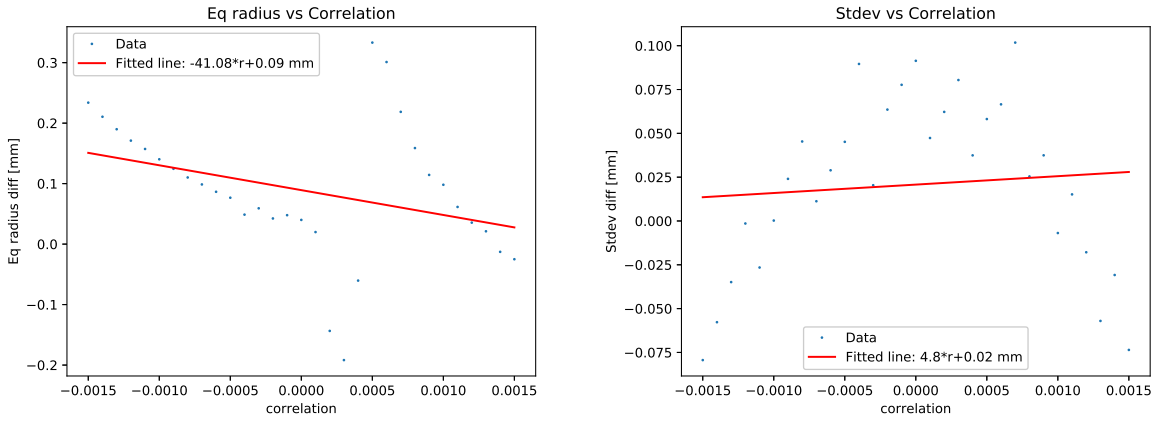

(a)

(b)

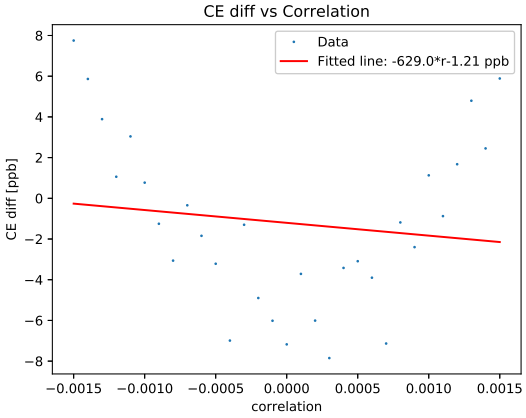

(c)

Figure 18: A scan over a linear momentum time correlation with Gaussian frequency distribution and longitudinal beam profile. Shown here are the difference between the recovered and actual (a) radial distribution [mm], (b) standard deviation [mm], (c) E-field correction. A linear fit is also done for each of the figures.

4.3.2 Quadratic correlation scan using optimized t_0 at max turn

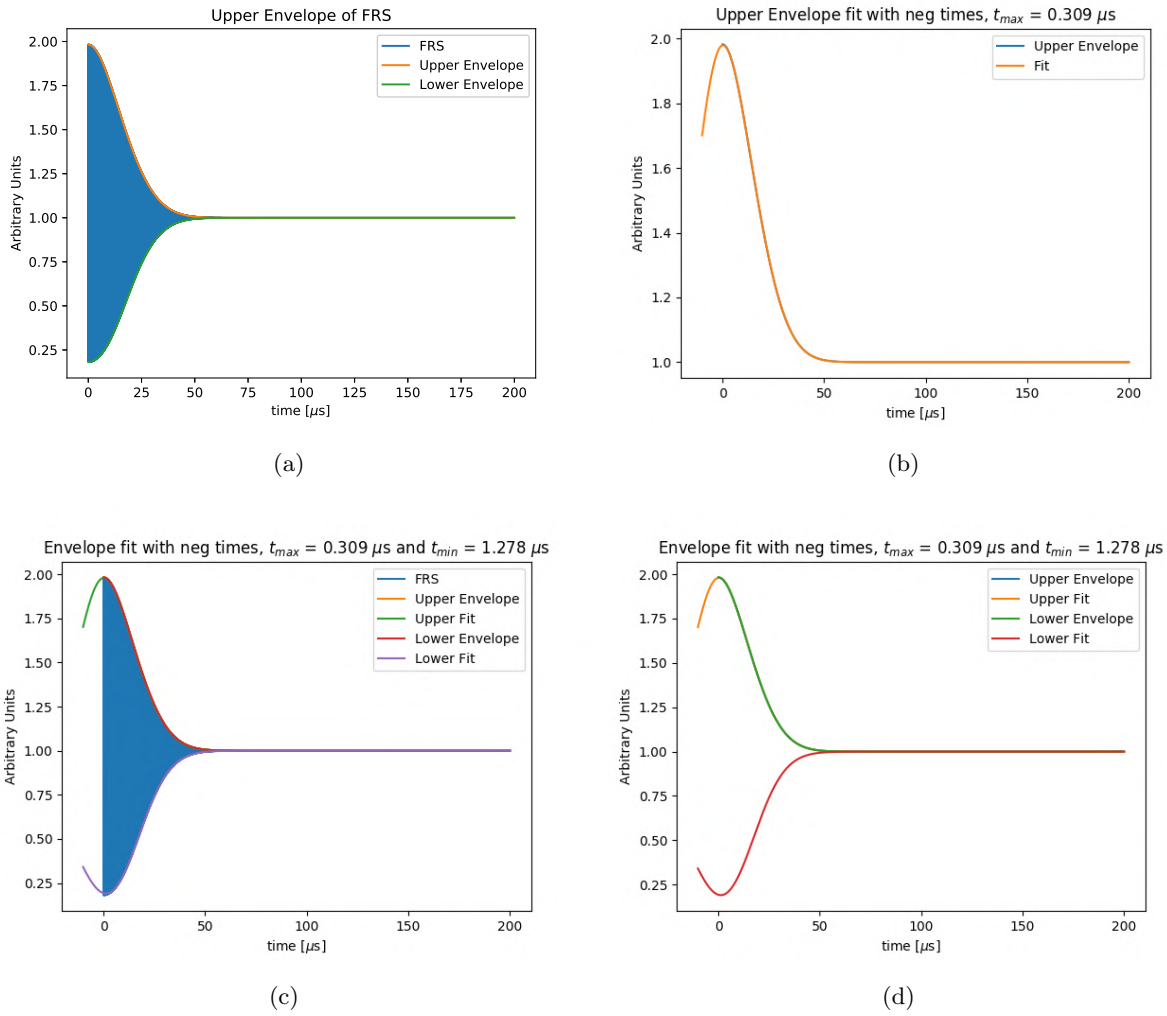

Figure 19: The envelope fit of the fast rotation signal for a quadratic correlation of 0.15%. (a) the upper and lower envelope and the FRS, (b) the upper envelope and the fit to it. (c) the upper and lower envelope and the fits together with the FRS, (d) the upper and lower envelope fits together.

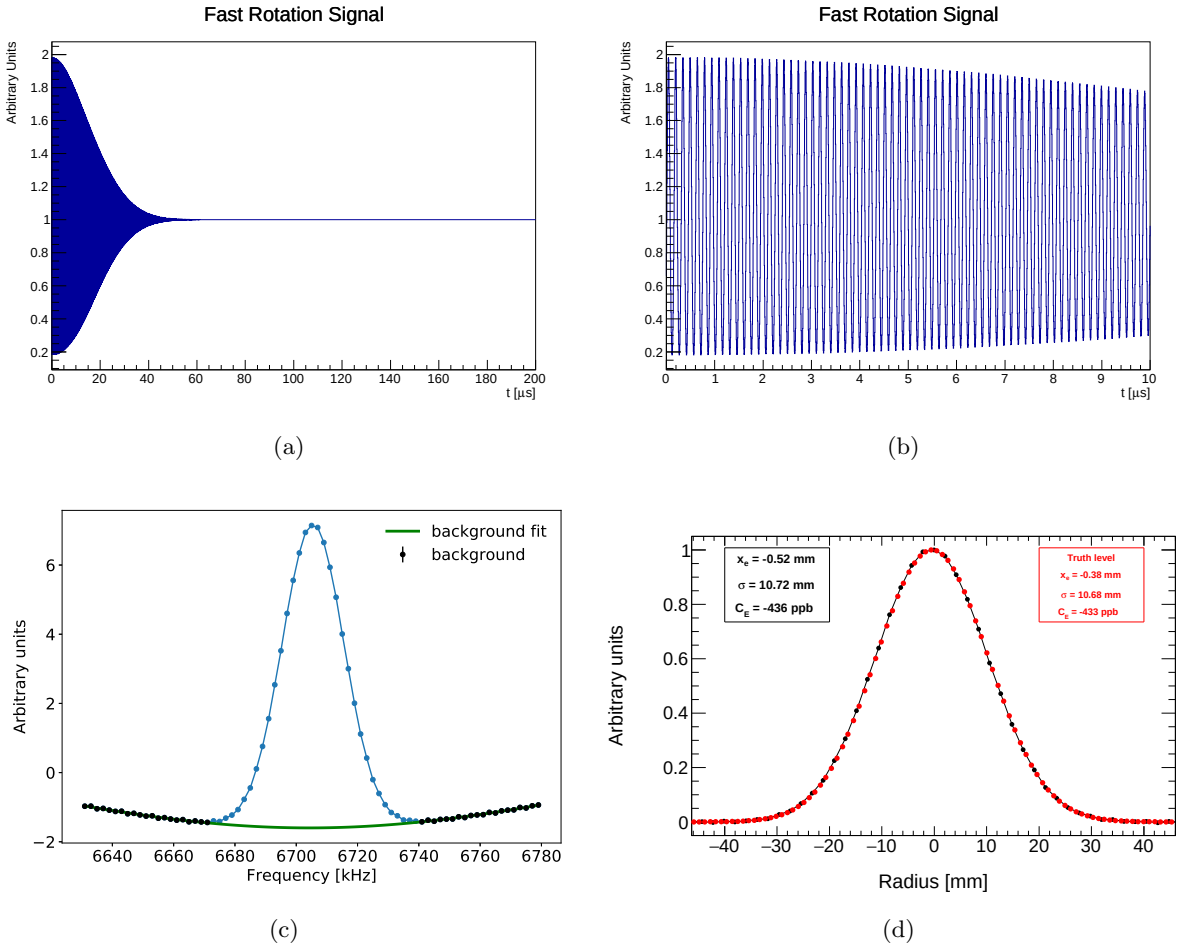

Figure 20: Fourier analysis of a fast rotation signal with Gaussian frequency distribution and longitudinal beam profile and a quadratic momentum time correlation of 0.15%. (a) fast rotation signal 0-200 μs, (b) fast rotation signal 0-10 μs, (c)background fit, (d) recovered radial distribution.

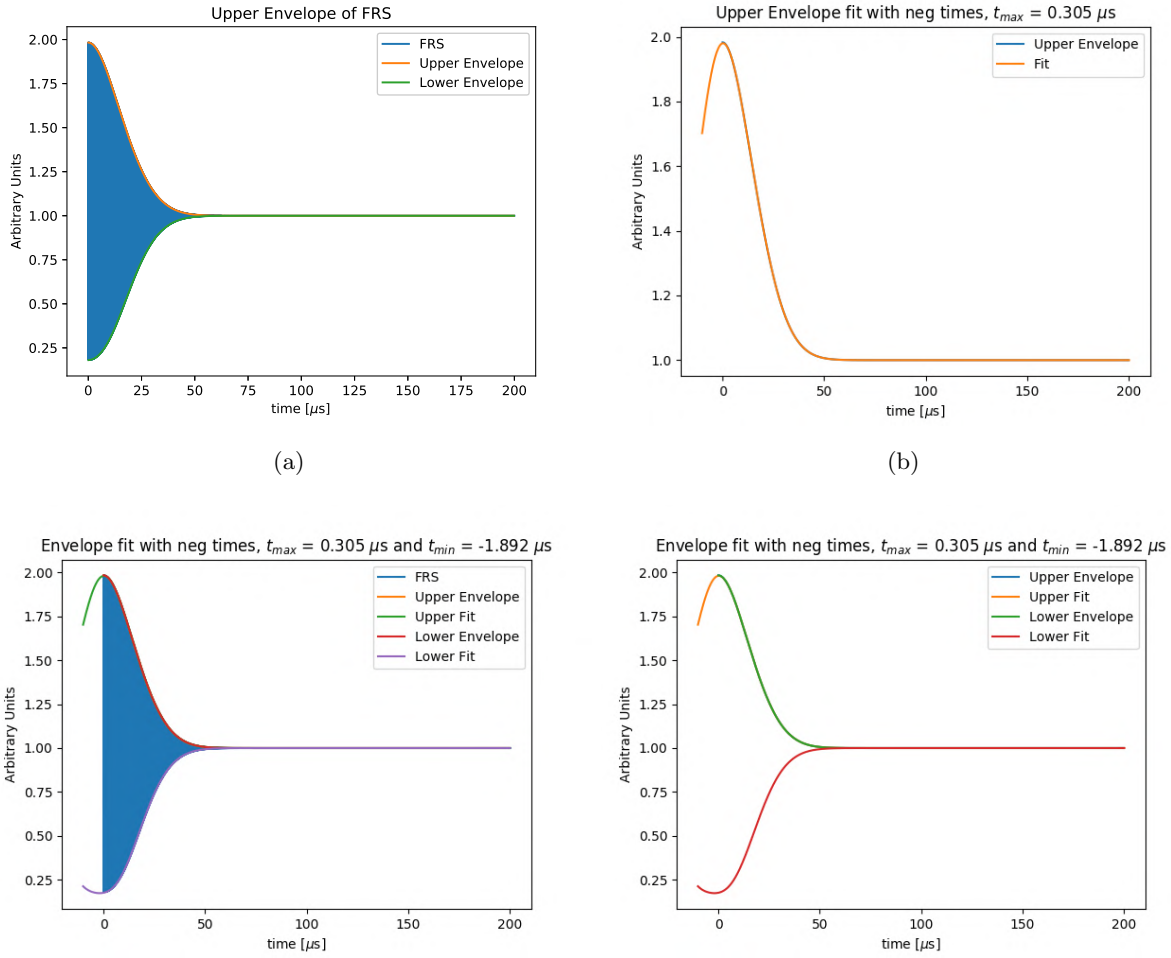

Figure 21: The envelope fit of the fast rotation signal for a quadratic correlation of -0.15%. (a) the upper and lower envelope and the FRS, (b) the upper envelope and the fit to it. (c) the upper and lower envelope and the fits together with the FRS, (d) the upper and lower envelope fits together.

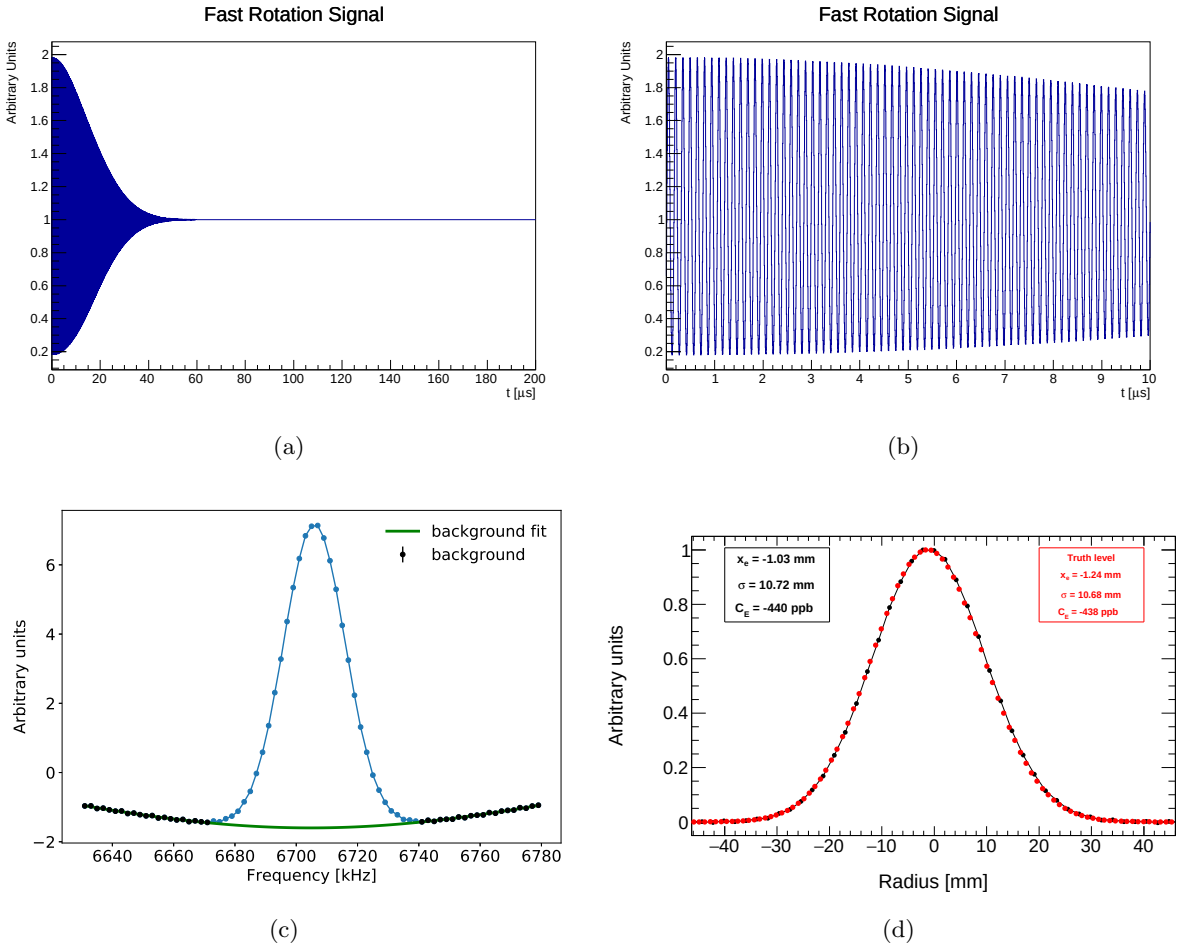

Figure 22: Fourier analysis of a fast rotation signal with Gaussian frequency distribution and longitudinal beam profile and a quadratic momentum time correlation of -0.15%. (a) fast rotation signal 0-200 μs, (b) fast rotation signal 0-10 μs, (c)background fit, (d) recovered radial distribution.

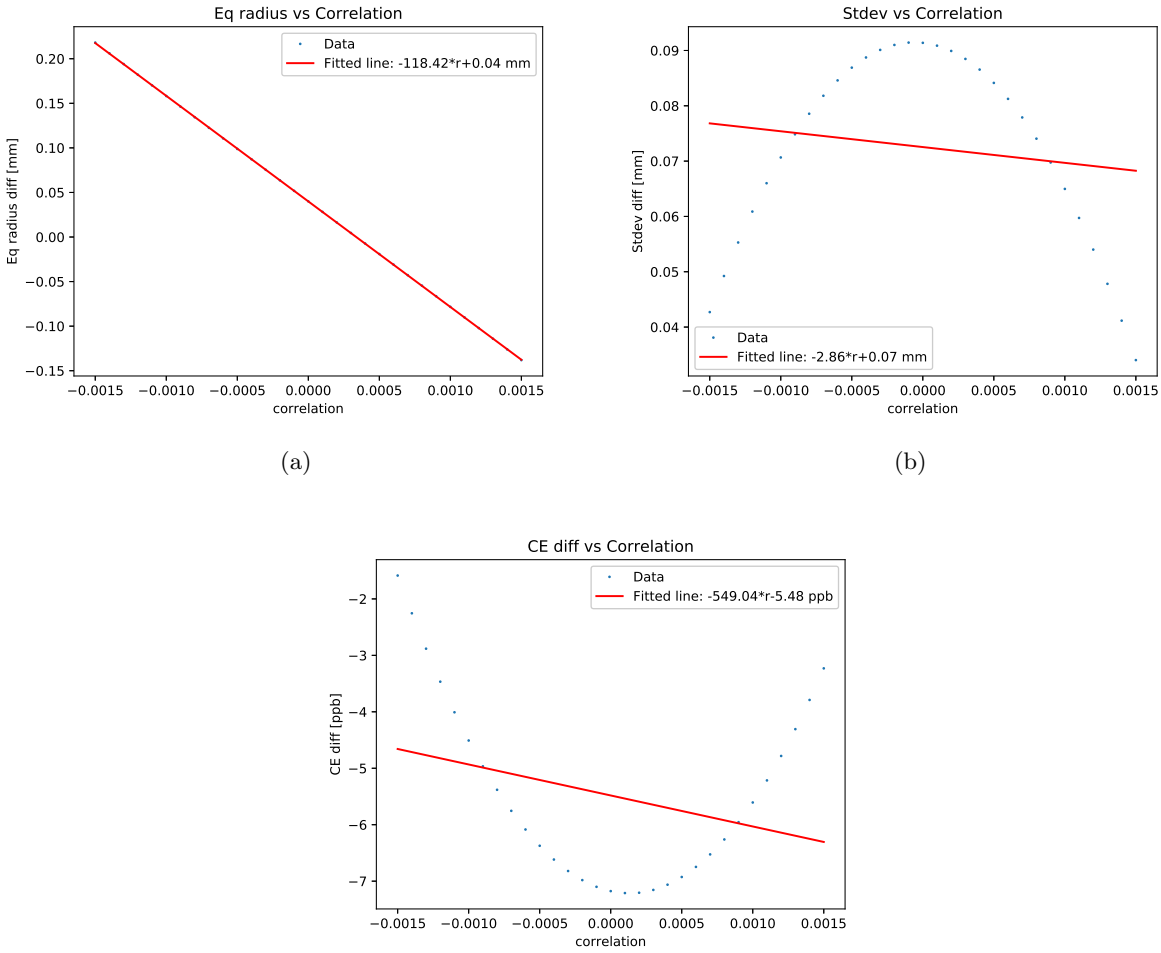

(a) (b)

(c)

Figure 23: A scan over a quadratic momentum time correlation with Gaussian frequency distribution and longitudinal beam profile. Shown here are the difference between the recovered and actual (a) radial distribution [mm], (b) standard deviation [mm], (c) E-field correction. A linear fit is also done for each of the figures.

4.3.3 Cubic correlation scan using optimized t_0 at max turn

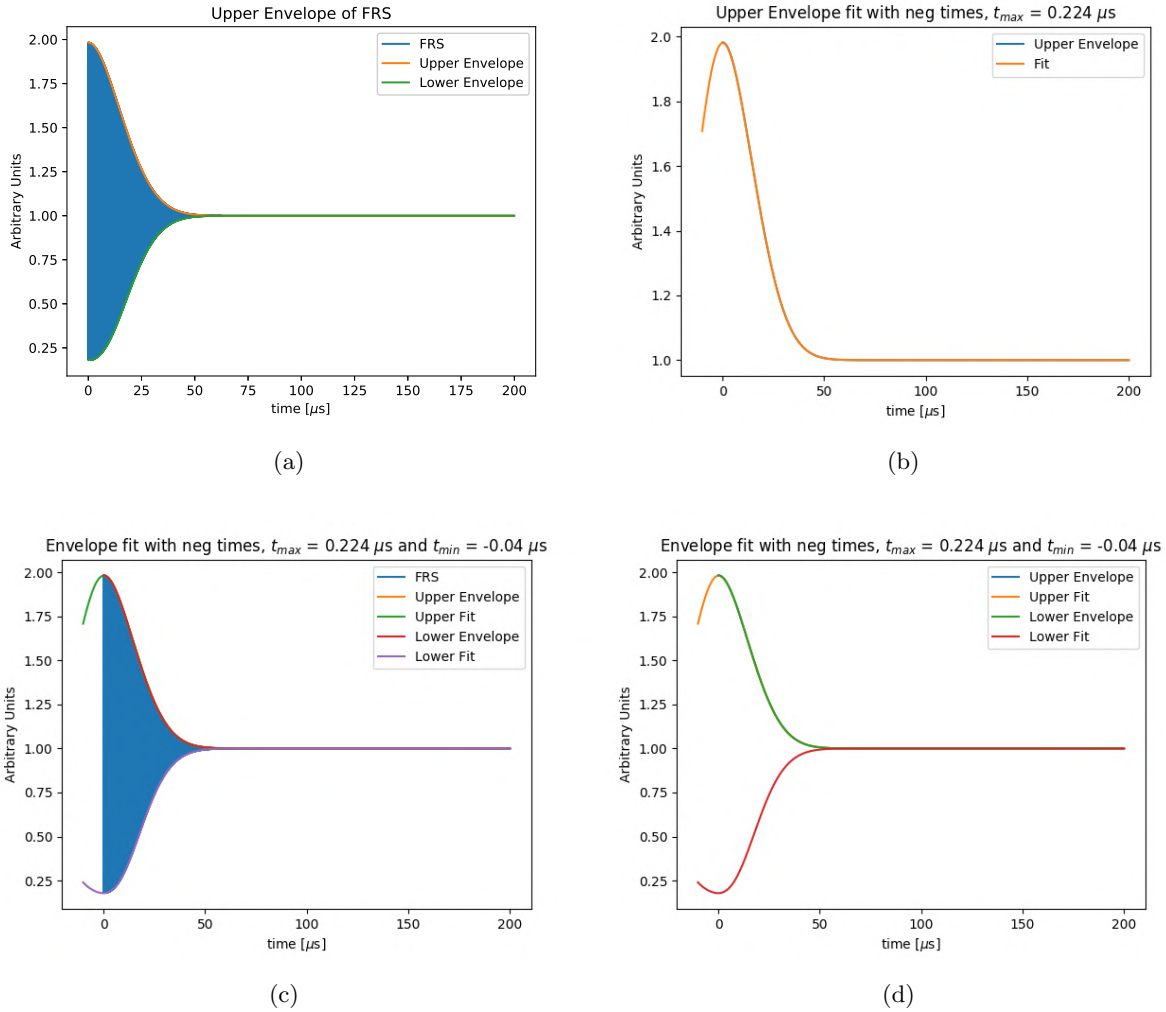

Figure 24: The envelope fit of the fast rotation signal for a cubic correlation of 0.15%. (a) the upper and lower envelope and the FRS, (b) the upper envelope and the fit to it. (c) the upper and lower envelope and the fits together with the FRS, (d) the upper and lower envelope fits together.

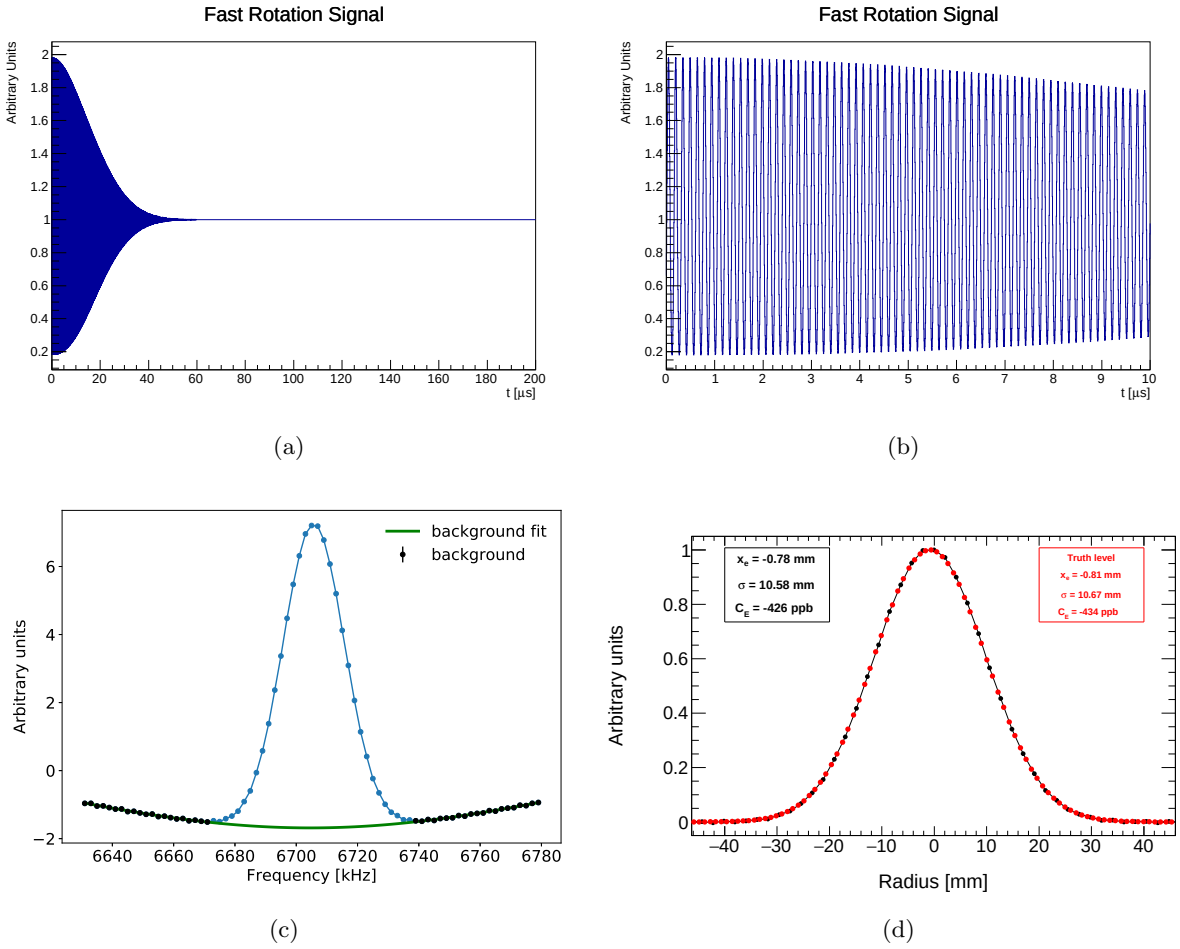

Figure 25: Fourier analysis of a fast rotation signal with Gaussian frequency distribution and longitudinal beam profile and a cubic momentum time correlation of 0.15%. (a) fast rotation signal 0-200 μs, (b) fast rotation signal 0-10 μs, (c)background fit, (d) recovered radial distribution.

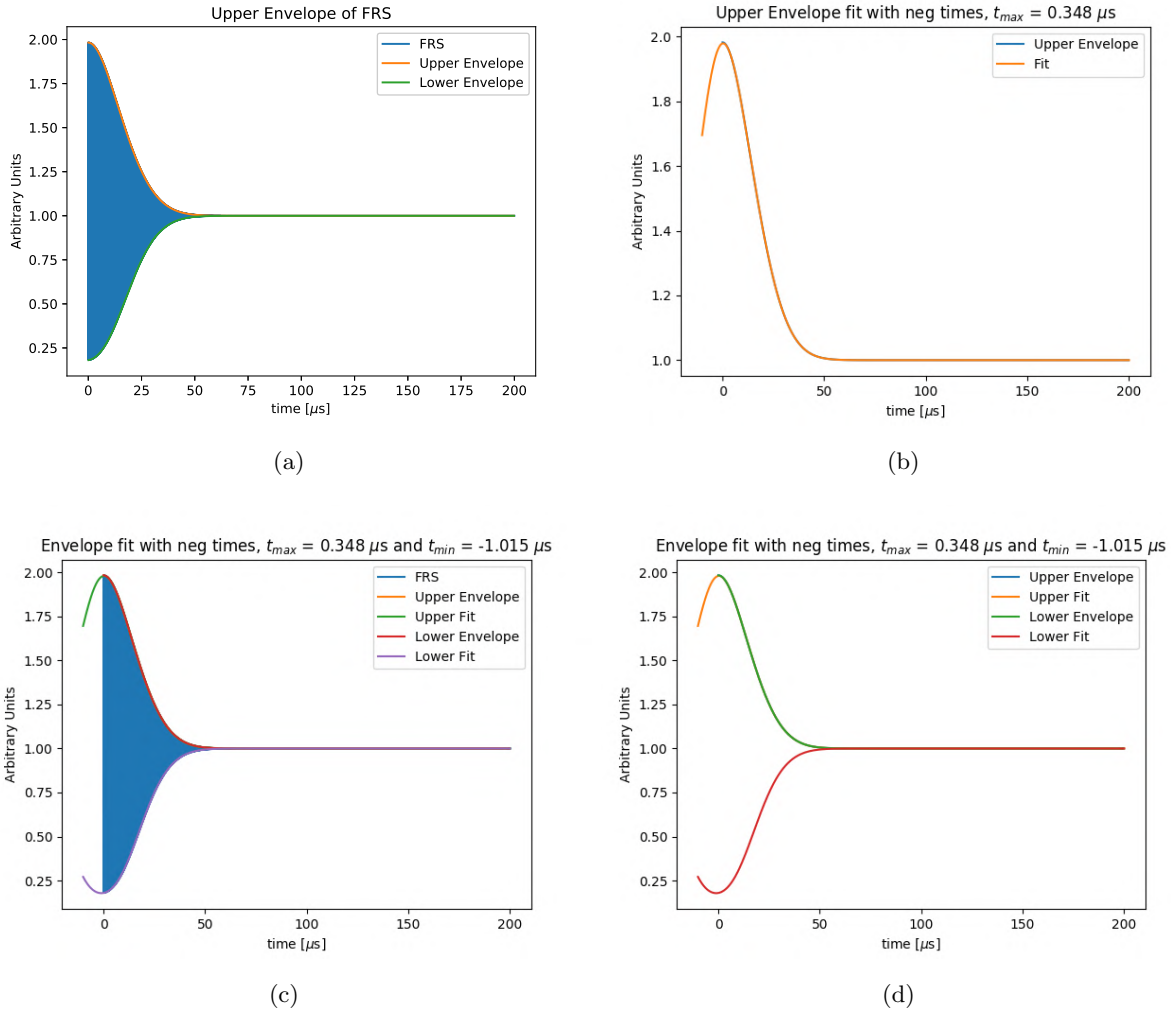

Figure 26: The envelope fit of the fast rotation signal for a cubic correlation of -0.15%. (a) the upper and lower envelope and the FRS, (b) the upper envelope and the fit to it. (c) the upper and lower envelope and the fits together with the FRS, (d) the upper and lower envelope fits together.

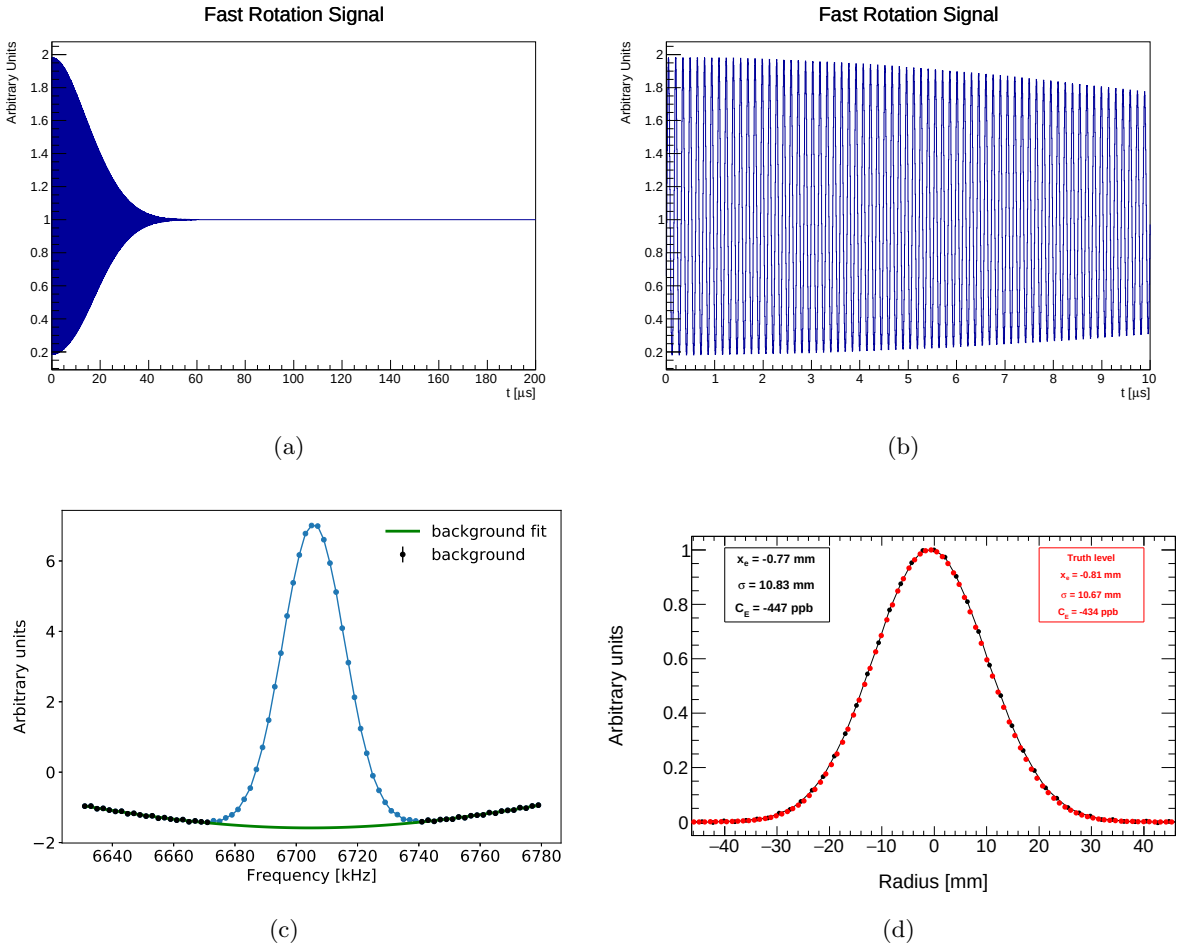

Figure 27: Fourier analysis of a fast rotation signal with Gaussian frequency distribution and longitudinal beam profile and a cubic momentum time correlation of -0.15%. (a) fast rotation signal 0-200 μs, (b) fast rotation signal 0-10 μs, (c)background fit, (d) recovered radial distribution.

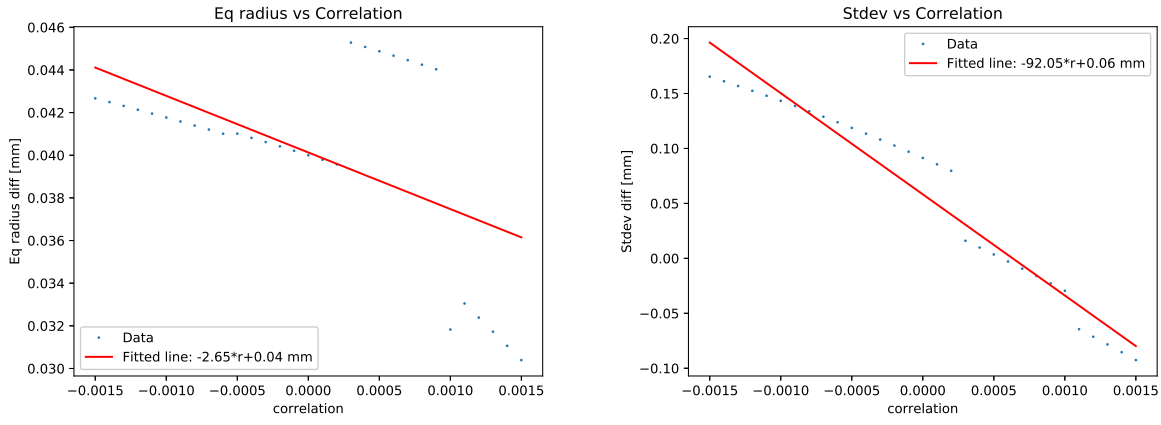

(a)

(b)

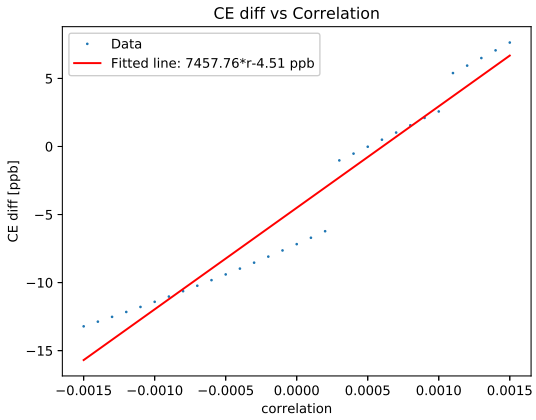

(c)

Figure 28: A scan over a cubic momentum time correlation with Gaussian frequency distribution and longitudinal beam profile. Shown here are the difference between the recovered and actual (a) radial distribution [mm], (b) standard deviation [mm], (c) E-field correction. A linear fit is also done for each of the figures.

4.3.4 Conclusion of correlation scan using optimized t_0 at max turn

We were able to recover the E-field correction within just 8 ppb for linear momentum time correlation of $\pm 0.15\%$ using the max of the fitted upper envelope. The linear momentum time correlation starting at the first turn recovered the E-field correction by as much as 100 ppb shown in section 4.2. The quadratic and cubic cases had max fitted envelopes around the first turn so were recovered nominally also within just 8 ppb. This is because with the Gaussian frequency distribution and beam profile the correlation for the quadratic and cubic cases were much less prominent than the linear case.

5 Outlook on real data

We have been able to account for the correlation for Monte Carlo using a Gaussian frequency distribution and longitudinal beam profile. There is still much more work to do before we can apply this to real data sets. In figure 29 an example of trying to apply this fit to real data is shown. The max value found from the upper envelope fit is at -5.277 μs. More Monte Carlo studies need to be done using more realistic conditions to determine if this is actually the proper point of symmetry for the dataset and to estimate the systematic uncertainty with the momentum time correlation.

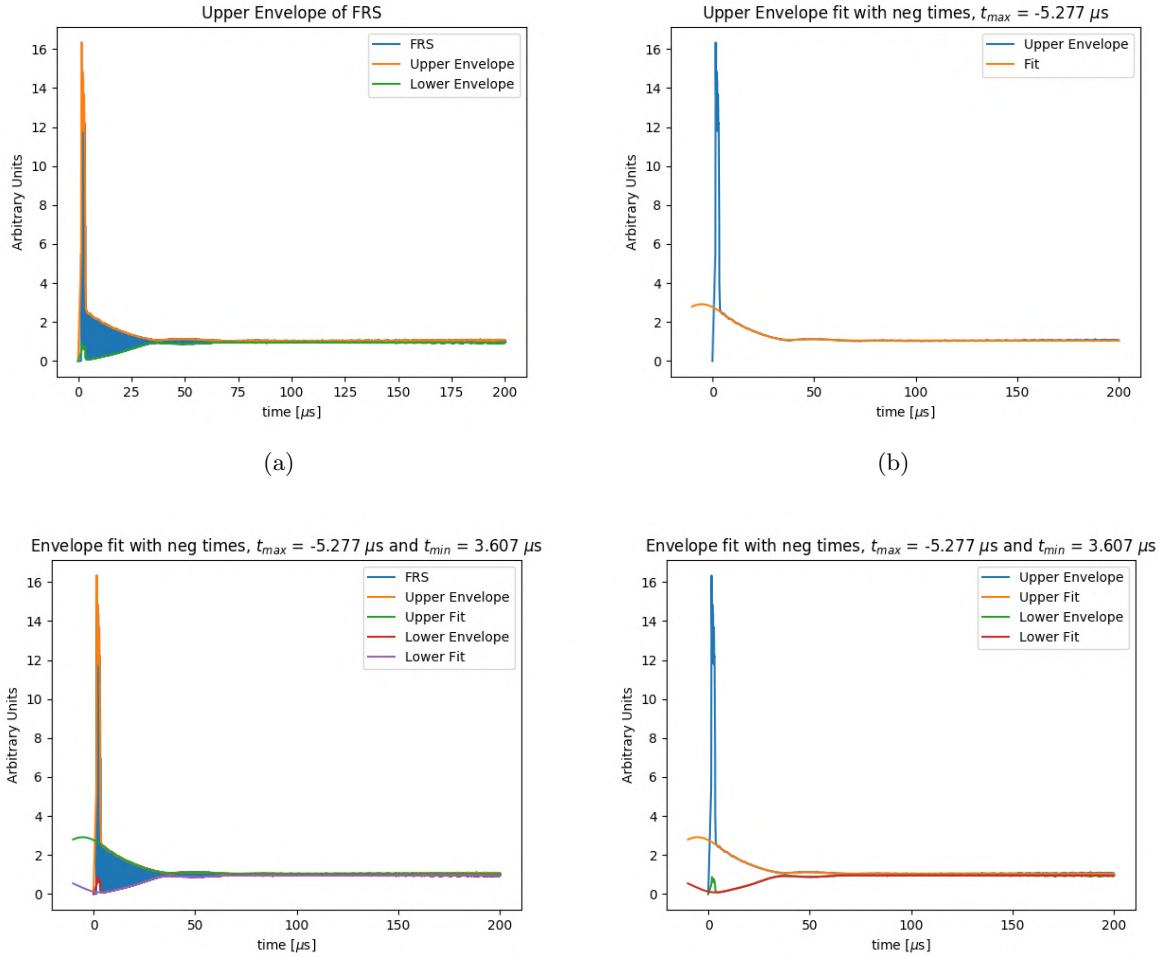

Figure 29: The envelope fit of the Run-1 60-hour data set. (a) the upper and lower envelope and the FRS, (b) the upper envelope and the fit to it. (c) the upper and lower envelope and the fits together with the FRS, (d) the upper and lower envelope fits together.

References

[1] A. Chapelain, J. Fagin, D. Rubin, D. Seleznev, *Cornell fast rotation Monte Carlo method and user guide*, GM2-doc-COMING-SOON

[2] A. Chapelain, J. Fagin, D. Rubin, D. Seleznev, *Cornell fast rotation Fourier method*, GM2-doc-18901

[3] A. Chapelain, D. Rubin, D. Seleznev, *Extraction of the Muon Beam Frequency Distribution via the Fourier Analysis of the Fast Rotation Signal*, E989 note 130, GM2-doc-9701

[4] A. Chapelain, J. Fagin, D. Rubin, D. Seleznev, *Cornell fast rotation Fourier analysis user guide*, GM2-doc-18460

[5] Y. Orlov et al., NIM A 482 (2002) 767-755.

[6] A. Chapelain, J. Fagin, D. Rubin, D. Seleznev, *On the background correction of the Cornell fast rotation Fourier analysis*, GM2-doc-19225-v1

[7] A. Chapelain, J. Fagin, D. Rubin, D. Seleznev, *Cornell fast rotation Fourier analysis performance study with toy Monte Carlo simulation*, GM2-doc-19132-v2

[8] A. Chapelain, J. Fagin, D. Rubin, D. Seleznev, *Extraction of the radial distribution of the stored muon beam for the Run–1 60–hour data set via the Cornell fast rotation Fourier method: estimation of the electric field correction to the anomalous spin precession frequency*, GM2-doc-19150-v3

[9] A. Chapelain, J. Fagin, D. Rubin, D. Seleznev, *Extraction of the radial distribution of the stored muon beam for the Run–1 9–day data set via the Cornell fast rotation Fourier method: estimation of the electric field correction to the anomalous spin precession frequency*, GM2-doc-19252-v4

[10] A. Chapelain, J. Fagin, D. Rubin, D. Seleznev, *Extraction of the radial distribution of the stored muon beam for the Run–1 end game data set via the Cornell fast rotation Fourier method: estimation of the electric field correction to the anomalous spin precession frequency*, GM2-doc-19258-v2

[11] A. Chapelain, J. Fagin, D. Rubin, D. Seleznev, *Extraction of the radial distribution of the stored muon beam for the Run–1 high kick data set via the Cornell fast rotation Fourier method: estimation of the electric field correction to the anomalous spin precession frequency*, GM2-doc-COMING-SOON